MOLECULAR AND CELLULAR BIOLOGY, Jan. 2007, p. 633–650 Vol. 27, No. 2
0270-7306/07/$08.00+0 doi:10.1128/MCB.00461-06

The Yeast PH Domain Proteins Slm1 and Slm2 Are Targets of Sphingolipid Signaling during the Response to Heat Stress▽†

Alexes Daquinag,[1]‡ Maria Fadri,[1]‡ Sung Yun Jung,[2] Jun Qin,[2] and Jeannette Kunz[1]*

Department of Molecular Physiology and Biophysics[1] and Department of Biochemistry and Molecular Biology,[2] Baylor College of Medicine, Houston, Texas 77030

Received 16 March 2006/Returned for modification 27 April 2006/Accepted 30 October 2006

The PH domain-containing proteins Slm1 and Slm2 were previously identified as effectors of the phosphatidylinositol-4,5-bisphosphate ($PI4,5P_2$) and TORC2 signaling pathways. Here, we demonstrate that Slm1 and Slm2 are also targets of sphingolipid signaling during the heat shock response. We show that upon depletion of cellular sphingolipid levels, Slm1 function becomes essential for survival under heat stress. We further demonstrate that Slm proteins are regulated by a phosphorylation/dephosphorylation cycle involving the sphingolipid-activated protein kinases Pkh1 and Pkh2 and the calcium/calmodulin-dependent protein phosphatase calcineurin. By using a combination of mass spectrometry and mutational analysis, we identified serine residue 659 in Slm1 as a site of phosphorylation. Characterization of Slm1 mutants that mimic dephosphorylated and phosphorylated states demonstrated that phosphorylation at serine 659 is vital for survival under heat stress and promotes the proper polarization of the actin cytoskeleton. Finally, we present evidence that Slm proteins are also required for the trafficking of the raft-associated arginine permease Can1 to the plasma membrane, a process that requires sphingolipid synthesis and actin polymerization. Together with previous work, our findings suggest that Slm proteins are subject to regulation by multiple signals, including $PI4,5P_2$, TORC2, and sphingolipids, and may thus integrate inputs from different signaling pathways to temporally and spatially control actin polarization.

Sphingolipids have emerged as key regulators of diverse cellular processes in eukaryotic cells (17, 18). Sphingolipids are major components of eukaryotic cell membranes, particularly the plasma membrane where they play important structural roles. More recently, it has been realized that sphingolipids also play vital regulatory roles. Studies in both mammalian cells and yeast cells have shown that sphingolipids, together with ergosterol (or cholesterol in mammalian cells), have the tendency to cluster together and form membrane microdomains, or lipid rafts, which are thought to act as platforms for the organization and regulation of signal transduction cascades and membrane trafficking events (50).

Specifically, in the yeast *Saccharomyces cerevisiae*, sphingolipids mediate diverse cellular functions required for cell growth, calcium homeostasis, actin cytoskeletal organization, endocytosis and secretion, and the cellular response to environmental stress (17, 18, 24). Signaling roles for sphingolipids during the response to heat stress conditions in yeast have been well established (10, 11). The de novo synthesis of sphingolipids is transiently induced in response to heat shock, causing a 2- to 100-fold increase in the sphingoid bases phytosphingosine (PHS) and dihydrosphingosine (DHS) and accumulation of their metabolites (19, 32, 58). PHS and DHS have been shown to act as signaling molecules and to directly activate a pair of functionally redundant protein kinases termed Pkh1 and Pkh2, the yeast homologs of mammalian phosphoinositide-dependent protein kinase 1 (9, 22). Pkh1 and Pkh2, in turn, phosphorylate and activate downstream protein kinases, including Pkc1, Sch9, and the related Ypk1 and Ypk2 (9, 29, 46, 47). Together, these kinases are thought to mediate sphingolipid-dependent signaling under heat stress and nonstress conditions. However, little is known about the targets of sphingolipid-dependent signaling or how those targets regulate the cellular machinery.

In addition to inducing an increase in de novo sphingolipid synthesis, heat stress also stimulates a transient increase in the synthesis of the lipid second messenger phosphatidylinositol-4,5-bisphosphate ($PI4,5P_2$) (16). $PI4,5P_2$ is a critical regulator of growth, actin cytoskeletal dynamics, and a variety of other cellular processes (55, 59). Interestingly, yeast mutants lacking $PI4,5P_2$ synthesis exhibit many of the same phenotypes as mutants lacking sphingolipid biosynthesis or Pkh1/2 function, including depolarization of the actin cytoskeleton and defects in cell wall integrity and endocytosis (1, 15, 16, 28). These findings suggested the possibility of cross talk between the two signaling pathways, and recent studies support a functional connection between $PI4,5P_2$ and sphingolipid signaling pathways. Specifically, deletion of *CSG2*, encoding the catalytic subunit of the enzyme that synthesizes the sphingolipid mannosylated inositol-phosphoceramide (MIPC), leads to intracellular accumulation of the complex sphingolipid inositol-phosphoceramide (IPC) and thereby causes calcium sensitivity (6, 56). Isolation and identification of yeast mutants that suppress the calcium-sensitive growth of the *csg2*Δ mutant subsequently identified genes involved in sphingolipid biosynthesis or signaling (5, 6, 61). In addition, these screens also identified a mutation in *MSS4*, the gene encoding the single essential PI4P 5-kinase that synthesizes $PI4,5P_2$ (5). These data imply a connection

* Corresponding author. Mailing address: Department of Molecular Physiology & Biophysics, Baylor College of Medicine, One Baylor Plaza, BCM335, RM T419, Houston, TX 77030. Phone: (713) 798-5797. Fax: (713) 798-3475. E-mail: jkunz@bcm.tmc.edu.

† Supplemental material for this article may be found at http://mcb.asm.org/.

‡ These two authors contributed equally to this work.

▽ Published ahead of print on 13 November 2006.

TABLE 1. *Saccharomyces cerevisiae* strains used in this study

Strain	Genotype	Source
W303a	*MAT***a** *ade2-1 trp1-1 can1-100 leu2-3,112 his3-11,15 ura3-1 GALs*$^+$	Lab collection
W303α	*MAT***a** *ade2-1 trp1-1 can1-100 leu2-3,112 his3-11,15 ura3-1 GAL*$^+$	Lab collection
BY4741	*MAT***a** *his3Δ1 leu2Δ0 met15Δ0 ura3Δ0*	Lab collection
95700	BY4741 except *SLM1-GFP-URA3*	Research Genetics
7502123	BY4741 except *SLM1-TAP-HIS3*	Open Biosystems
7501161	BY4741 except *SLM2-TAP-HIS3*	Open Biosystems
RH3804	*MAT*α *lcb1-100 trp1 leu2 ura3 lys2 bar1*	H. Riezman, University of Geneva, Geneva, Switzerland
*erg24*Δ strain	BY4741 except *erg24*::*kanMX*	38
JK502	W303a except *slm1*::*kanMX*	19
JK506	W303a except *slm2*::*HIS3*	19
JK515	W303a except *slm1*::*kanMX slm2*::*HIS3* carrying p*416GPD-slm1-3*	This study
JK520	W303a except *slm1*::*kanMX slm2*::*HIS3*/pAS25::*SLM1*	This study
*ypc1*Δ strain	W303α except *ypc1*::*kanMX TRP1*	This study
*sur1*Δ strain	W303α except *sur1*::*kanMX TRP1*	This study
*lcb3*Δ strain	W303α except *lcb3*::*kanMX TRP1*	This study
*lcb4*Δ strain	W303α except *lcb4*::*kanMX TRP1*	This study
*fen1*Δ strain	W303α except *fen1*::*kanMX TRP1*	This study
*csg2*Δ strain	W303α except *csg2*::*kanMX*	This study
*ipt1*Δ strain	W303α except *ipt1*::*kanMX*	This study
*pkh1-ts pkh2*Δ strain	*pkh1-D398G pkh2*::*LEU2*	28
YPT40	*MAT***a** *ypk1-1*^{ts}*–HIS3 ypk2*::*TRP1 ade2-101 his3-200 leu2-1 lys2-801 trp1-1 ura3-52*	8
SH121	JK9-3d**a** *ade2*/*tor2*::*ADE2*/YCplac111::*tor2*-21	M. Hall

between sphingolipid and PI4,5P_2 signaling pathways, but the molecular mechanisms of how this might be achieved and the point(s) of convergence between the two pathways have remained elusive.

One possible way in which sphingolipids may intersect with the PI4,5P_2 signaling pathway is by modulating the activation or localization of targets of PI4,5P_2-dependent signaling. The recently identified redundant PI4,5P_2 effectors Slm1 and Slm2 are essential for growth and actin cytoskeletal organization and require their PH domains for targeting the plasma membrane in a PI4,5P_2-dependent manner (3, 20). Because Slm1 and Slm2 colocalize with the lipid raft-associated protein Pma1 (20), they are good candidates for linking sphingolipid and PI4,5P_2 signaling pathways. Furthermore, Slm1 and Slm2 also interact with and are regulated by the TORC2 signaling complex (3, 20), which controls growth and actin cytoskeleton organization in response to a variety of stress conditions, including heat and cell wall and nutrient stress. *SLM1* was also isolated genetically as a dosage suppressor of the TORC2 component Avo3 (27). Interestingly, TORC2 components, including Tor2 and Avo3, were identified among the collection of mutants that suppress the calcium-sensitive growth of the *csg2*Δ mutant (5, 6, 61), suggesting a functional link between Slms, TORC2 and sphingolipid metabolism. Taken together, these findings raise the possibility that Slm1 and Slm2 may be a point of convergence between sphingolipid, phosphoinositide, and TORC2 signaling pathways and suggest that modulation of Slm function in response to environmental signals could be an efficient way of modulating the output of essential pathways to coordinate the cellular response to various stress conditions.

In the present study, we show that Slm proteins and sphingolipids cooperate to promote cell survival by regulating cell growth and proper actin polarization. We demonstrate that Slm phosphorylation during heat stress is dependent on the activity of the sphingolipid-regulated protein kinases Pkh1 and Pkh2. Phosphorylation of Slm is antagonized by the Ca^{2+}/calmodulin-dependent protein phosphatase calcineurin, which binds Slm1 and Slm2 via a conserved calcineurin-binding motif present in their C termini. Genetic evidence places Slm1 in a branch of the Pkh1 and Pkh2 pathway and suggests that Slm proteins provide a subset of Pkh-dependent functions required for proper actin polarization. Furthermore, Slm proteins and Pkh kinases are required for the trafficking of the raft-associated arginine permease Can1 to the plasma membrane, a process that is dependent on de novo sphingolipid biosynthesis and polymerized actin. Together with results obtained in previous studies, our data suggest that Slm1 and Slm2 link inputs from multiple signaling pathways to regulate actin polarization in response to various environmental stimuli.

MATERIALS AND METHODS

Materials, strains, and plasmids. Protease inhibitor mix lacking EDTA was obtained from Roche Immunochemicals. G418 and *Pfx* polymerase were from Invitrogen. Primestar polymerase was from Takara Mirus Bio. (Madison, WI). Glutathione *S*-transferase (GSH)-conjugated agarose beads were from Clontech, immunoglobulin G (IgG)-conjugated Sepharose beads were from Sigma-Aldrich, and mouse monoclonal antihemagglutinin (anti-HA) IgG conjugated to Sepharose beads was from Babco. Mouse monoclonal anti-GST antibodies were from Sigma-Aldrich, mouse monoclonal anti-HA antibodies were from Babco, rabbit polyclonal anti-TAP antibodies were from OpenBiosystems, Cy2-conjugated goat anti-mouse IgG and Cy3-conjugated goat anti-rabbit IgG were from Jackson ImmunoResearch, and Alexa594-conjugated phalloidin was from Molecular Probes. Molecular mass standards were from Bio-Rad Laboratories. Myriocin and PHS were purchased from Sigma (St. Louis, MO). Myriocin was dissolved in ethanol at a stock concentration of 2 mg/ml and was stored at 4°C, whereas PHS was dissolved in ethanol at 15 mM and stored at −20°C. FK506 was obtained from AG Scientific (San Diego, CA) and was dissolved in 90% ethanol–10% Tween 20 at a stock concentration of 10 mg/ml and stored at −20°C. Antiphosphoserine (Q5) and antiphosphothreonine (Q7) antibodies were purchased from QIAGEN (Hilden, Germany).

S. cerevisiae strains used are listed in Table 1. Yeast strains from the yeast deletion collection were purchased from OpenBiosystems and backcrossed twice

into the W303 strain background. Plasmids YCpG22-PKH1 (*GAL1*p-*PKH1 TRP1)*, pJK702 (*GAL1*p-*HA*$_2$-*SLM1* in pAS25 YCplac33 *CEN URA3*), and pJK708 (*6HIS-SLM2* in pET28a) were previously described (18, 28). Plasmids pJK714 (*GST-SLM1*$_{\Delta CNA}$ in pEGKT or pAS25) and pJK715 (*GST-SLM2*$_{\Delta CNA}$ in pEGKT) containing Slm1 and Slm2 deletion mutants lacking the calcineurin binding site were constructed as follows by PCR amplification using the following primer combinations: Slm1-CN-For (5′-CTACTACTCGAGTTATTCATCATTTTCTACCATTGTGC) and Slm1-CN-Rev (5′-CTACTACTCGAGTTATTGATCTTGTAATTCAGAATCAT); Slm2-CN-For (5′-CTACTACTCGAGTTACGTATGTTGCTCATTAGTTACC) and Slm2-CN-Rev (5-CTACTACTCGAGTTAATTCTGAATTTGTGAATCATTCG). Ser569 in Slm1 was mutagenized using the following primer combinations: Slm1S659A-For (5′-ACATCCATGTCTGCATTACCTGATACT) and Slm1S659A-Rev (5′-AGTATCAGGTAATGCAGACATGGATGT); Slm1S659D-For (5′-ACATCCATGTCTGACTTACCTGATACT) and Slm1S659D-Rev (5′-AGTATCAGGTAAGTCAGACATGGTTGT). Underlining indicates nucleotide changes in the mutants. All PCR products were digested with XhoI (site contained within primer sequences) and cloned either into the SalI site in the vector pEGKT, resulting in in-frame fusion with GST, into the SalI site of pAS25, resulting in in-frame fusion with HA, or into the XhoI site of vector p425GPD. DNA sequences were confirmed by sequencing.

General genetic manipulations. Wild-type yeast strains and temperature-sensitive mutants were grown at 26°C unless otherwise indicated. Media are described elsewhere (49). Unless otherwise indicated, YPD and SD medium contained 2% glucose, whereas YPG and SG medium contained 2% galactose and 2% raffinose as the carbon source. Strain construction followed standard methods (49). Yeast cells were transformed by the lithium acetate procedure (30), and transformants were selected on SD medium lacking the appropriate amino acid supplement for maintenance of the plasmid marker.

Quantitation of myriocin and canavanine sensitivity. Myriocin and PHS were stored as stock solutions at −20°C and were prewarmed to room temperature (RT) before being added to media at the desired concentration. Canavanine (10 mg/ml in water) was stored at 4°C. Sensitivity of the indicated yeast strains to drugs was tested by spotting serial dilutions (1:10) of yeast strains adjusted to an A_{600} of 1.0 on YPD plates supplemented with various concentrations of myriocin, PHS, or drug vehicle alone. For canavanine sensitivity, cultures were spotted on plates lacking arginine but containing canavanine (0.5 or 1 μg/ml). Plates were incubated at the appropriate temperatures for 3 to 4 days before photography.

Genetic interaction between *slm1*Δ strains and strains with mutations in the sphingolipid biosynthetic pathway. Doubly heterozygous diploids were generated by crossing haploid strains and selecting for the presence of appropriate markers. To obtain double mutants, the *slm1*::*kanMX* deletion strain in the W303 genetic background was mated with isogenic strains containing deletions in genes coding for enzymes in the sphingolipid biosynthesis pathway (Fig. 1). Diploids were sporulated at 26°C, and tetrads were dissected, allowed to germinate at 26°C on YEPD medium, and scored for G418 resistance or the presence of auxotrophic markers. Only tetrads that yielded four viable progeny of which two were G418 resistant and two were G418 sensitive were analyzed, with G418-resistant segregants being assumed to be double mutants. To test for synthetic sickness, growth of the wild type and isogenic single- and double-mutant segregants was assayed by diluting overnight cultures to an A_{600} of 1.0 and spotting serial 10-fold dilutions of the strains onto YPD plates. Plates were incubated at 26°C or 38°C, and growth was scored after 3 to 4 days.

Detection of Slm phosphorylation by immunoprecipitation and Western blotting. Slm phosphorylation was generally assayed in strains containing chromosomally expressed Slm1-TAP and Slm2-TAP under the control of their endogenous promoter. Slm1-TAP was functional, because a yeast strain containing *SLM1-TAP* in combination with a deletion in *SLM2* was viable and grew like the wild-type strain (data not shown). Cultures were grown in YPD medium at 26°C to and A_{600} of 1.0 and were then treated with vehicle alone, chemical inhibitors (myriocin, 2 μg/ml; FK506, 2 μg/ml; BAPTA [1,2-*bis*(*o*-aminophenoxy)ethane-*N*,*N*,*N*′,*N*′-tetraacetic acid], 10 mM), or other compounds (PHS, 10 μM; $CaCl_2$, 100 mM) for an additional 45 min. For heat shock experiments, cultures were then divided into aliquots and incubated with shaking at either 26°C or 38°C for various periods. To prepare whole-cell extracts, yeast cells were collected by centrifugation for 4 min at 3,000 rpm and 4°C, resuspended in lysis buffer (50 mM Tris-HCl [pH 7.5], 50 mM NaCl, 0.1 mM EDTA, 0.1% NP-40, 10% glycerol, supplemented with complete protease inhibitor mix and 2 mM concentrations of the phosphatase inhibitors NaF, $NaVO_3$, and β-glycerophosphate), lysed with glass beads in a bead beater (six times for 30 s each at 4°C; BioSpecs), and clarified by microcentrifugation (500 × *g*, 15 min at 4°C). TAP-tagged Slm proteins were purified as described elsewhere (25) from 5 mg whole-cell extract (diluted 1:5 with lysis buffer), using an IgG-Sepharose column followed by three washing steps with ice-cold lysis buffer. Bead-bound immune complexes were solubilized in sodium dodecyl sulfate-polyacrylamide gel electrophoresis (SDS-PAGE) sample buffer, immediately boiled for 5 min in a water bath, and then clarified by brief centrifugation in a microcentrifuge before resolution by SDS-PAGE.

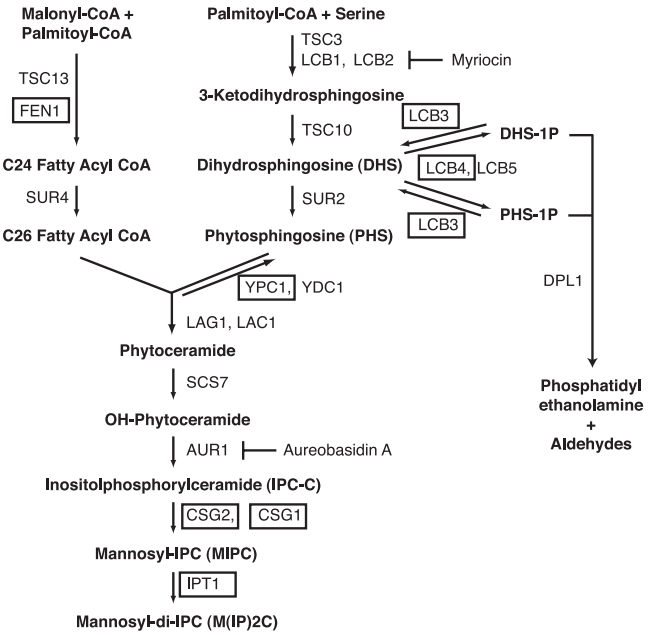

FIG. 1. Pathways involved in sphingolipid biosynthesis in *S. cerevisiae*. A schematic overview of the sphingolipid biosynthetic and degradation pathways is shown. Steps in sphingolipid biosynthesis blocked by chemical inhibitors myriocin and aureobasidin A are indicated. Deletion mutants used to test for genetic interactions with the *slm1*Δ mutant are boxed.

To compare Slm phosphorylation in the wild-type and *pkh1ts pkh2*Δ, *ypk1-ts ypk2*Δ, and *tor1*Δ *tor2*Δ mutant strains, *SLM1* was expressed from the *GAL1* promoter as fusion proteins with a double-HA epitope at the N terminus (pAS25, *CEN URA3*). To analyze phosphorylation of the Slm1$_{\Delta CN}$ mutant, the wild type and the mutant Slm1 variants were expressed in strain W303 as N-terminal TAP fusion proteins from a centromere-based plasmid under the control of the *GAL1* promoter. In all cases, cells were cultivated in raffinose-containing selective medium to an A_{600} of 1.0, followed by a 2.5-h galactose induction. Glucose was then added to a 2% final concentration to stop protein expression, and cells were incubated for another 30 min at 26°C. Cells were then divided into 50-ml aliquots and heat shocked by incubation at 38°C for various periods. Cell extract preparation and TAP purification and analysis were performed as described above. HA-tagged Slm1 was purified from extracts of wild-type and *pkh1ts pkh2*Δ mutant strains using anti-HA-Sepharose affinity beads. The phosphorylation status of Slm fusion proteins was analyzed by Western blotting using antiphosphoserine (Q5) and antiphosphothreonine (Q7) antibodies essentially following the manufacturer's protocol. Detection of tagged proteins by anti-HA or anti-TAP antibodies was as described previously (20). Western blots were sequentially probed with each antibody with stripping in between. Western blots were developed using a commercial chemiluminescence detection system (Renaissance; PerkinElmer Life Sciences, Boston, MA) and X-ray film (Biomax MR; Eastman Kodak, Rochester, NY). Quantitation was performed in two ways. First, enhanced chemiluminescence (ECL) Western blots were exposed to ECL reagents for various periods (10 s to 8 min), and for each set of experiments (control/PHS/myriocin, control/$CaCl_2$/BAPTA/FK506, and control/Slm1$_{\Delta CN}$) the same exposures in the linear range were digitized and quantitated by densitometry using the Image Gauge 4.0 program. Quantitation was also performed with samples that were independently analyzed by SDS-PAGE and by quantitative Western blot analysis using primary antibodies and Alexa Fluor IR680-conjugated anti-rabbit antibody. Blots were analyzed with an Odyssey infrared imaging system (Licor Biosciences, Lincoln, NE). Both quantitation methods gave qualitatively the same result. However, it should be noted that between independent experiments, some variability in the magnitude of change in phosphoserine and phosphothreonine levels using Q5 and Q7 antibodies was

observed that may reflect the differences in basal phosphorylation levels at time zero.

Expression and purification of proteins in *Escherichia coli* and GST pull-down assays. All proteins were expressed in *E. coli* BL21(λDE3) as GST or His_6 fusion proteins and purified on GSH-conjugated and Ni^{2+}-chelating agarose beads, respectively, following the manufacturer's instructions. In vitro transcription and translation and labeling of proteins with [^{35}S]Easy Tag Express protein labeling mix (NEN Life Science Products) was performed using the Promega TNT T7 quick coupled transcription/translation system. *CNA1* cloned into vector TNT521 (20) was used as a DNA template in the reactions. Pull-down assays using radioactively labeled Cna1 and Slm1, Slm2, or deletion variants thereof were performed as described previously (20).

Proteomic analysis of Slm1 phosphorylation. Mass spectrometric identification of Slm1 phosphorylation was done as described before (33) with a minor modification. TAP-Slm1 protein was purified from heat-shocked (90 min, 38°C) wild-type cells as described above, separated by SDS-PAGE, and visualized by Coomassie brilliant blue staining. The Coomassie-stained protein band was excised and destained with 50 mM ammonium bicarbonate solution in 50% methanol. Gel pieces were washed in high-pressure liquid chromatography (HPLC) water overnight and digested with either 100 ng of trypsin or 100 ng of AspN in 50 mM NH_4HCO_3 (pH 8.5) for 4 h. After digestion, peptides were extracted by addition of 200 μl of acetonitrile, and supernatants were dried in a Speed-Vac dryer (Thermo Savant, Holbrook, NY). Each sample was then dissolved in 20 μl of a 5% methanol/95% water/0.1% formic acid solution and injected into a Surveyor HPLC system (ThermoFinnigan, Waltham, MA) using an autosampler. A C_{18} column (100 mm by 75 μm, 5 μm, 300-Å pore diameter; PicoFrit; New Objective, Woburn, MA) with mobile phases A (0.1% formic acid in water) and B (0.1% formic acid in methanol) was used with a gradient of 10 to 80% mobile phase B over 10 min followed by 80% B for 10 min at a flow rate of 200 nl/min. Peptides were directly electrosprayed into the mass spectrometer (Finnigan LTQ; ThermoFinnigan, San Jose, CA) using a nanospray source. LTQ were operated in the data-dependent mode, acquiring fragmentation spectra of the top 20 strongest ions. All tandem mass spectrometry (MS/MS) spectra were searched against the National Center for Biotechnology Information nr protein sequence database with the specification of serine, threonine, or tyrosine phosphorylation using the BioWorks database search engine (BioWorksBrowser version 3.2; Thermo Electron, Waltham, MA). Phosphorylated peptides were identified based on stringent BioWorksBrowser filtering criteria (a peptide probability of $>5 \times 10^{-5}$ and an Xcorr score of >4.0) and were manually examined for consecutive b- or y- ions to eliminate false positives.

Immunofluorescence techniques and actin depolymerization. Cells were prepared for immunofluorescence experiments as described previously (20). Green fluorescent protein (GFP) experiments in living cells were performed using cells grown in selective media (selecting for maintenance of chromosomal or plasmid-borne fusions) and mounted for viewing in 1% low-melting-point agarose. To investigate the role of the actin cytoskeleton in Can1 plasma membrane delivery, cells expressing GFP-Can1 from a low-copy-number vector (40) were treated with latrunculin A (5 μM) to depolymerize the actin cytoskeleton, and Can1 localization was visualized after various times. All cells were viewed using a 100× plan oil-immersion lens (numerical aperture, 1.4). Images were acquired with the use of a DeltaVision deconvolution microscope (Applied Precision, Mississauga, Ontario, Canada) and analyzed as described previously (20).

Scoring of actin cytoskeletal polarization. Actin polarization was examined in small- and medium-budded cells (~100 to 150 cells were analyzed in each case) as described previously (20). The actin cytoskeleton was considered polarized if six or fewer actin patches were localized in the mother cells, patches were concentrated at the bud neck, and actin cables were polarized. Cells with the majority of actin patches polarized to the bud and the bud neck and containing polarized actin cables were classified as partially polarized. Cells with more actin patches in the mother cell than in the bud were classified as depolarized.

RESULTS

***SLM1* deletion confers supersensitivity to myriocin.** Previously we demonstrated that Slm1 and Slm2 localize to characteristic plasma membrane subdomains that are enriched in the H^+-ATPase Pma1 (20). Because Pma1 is a well-documented lipid raft protein (4), this raised the questions of whether Slm proteins are also components of raft-based microdomains and whether their function is modulated by sphingolipids. Myriocin sensitivity has often been used as a readout to screen for and identify novel components of the sphingolipid signaling pathway in yeast (53). Myriocin blocks de novo synthesis of sphingolipids by specifically inhibiting Lcb1 (Fig. 1), the enzyme that catalyzes the first committed step in sphingolipid biosynthesis. To begin to examine a potential relationship between Slm proteins and sphingolipids, we tested whether myriocin affects growth of yeast cells lacking *SLM1* or *SLM2*.

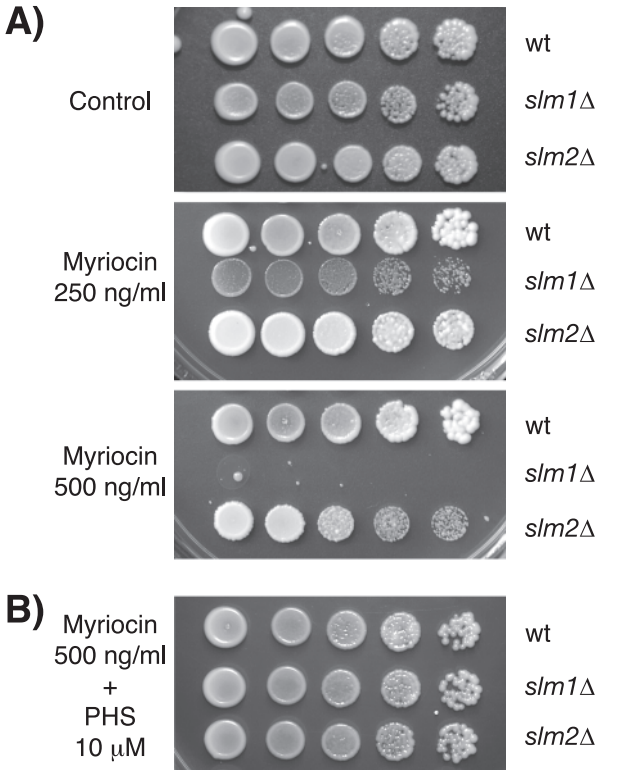

FIG. 2. Deletion of *SLM1* confers supersensitivity to myriocin. (A) Isogenic wild-type, *slm1*Δ, and *slm2*Δ mutant strains were grown to stationary phase in YPD medium, and serial dilutions of cultures were spotted on YPD plates containing either drug vehicle alone or the indicated concentrations of myriocin. (B) Addition of exogenous PHS (10 μM) to YPD plates containing 0.5 μg/ml myriocin rescues growth of the *slm1*Δ mutant. All plates were incubated at 30°C and photographed after 3 days.

In agreement with earlier findings (53), myriocin inhibited the growth of wild-type cells in a dose-dependent manner, with 2 μg/ml being the lowest concentration that can completely inhibit growth (data not shown). Compared to the wild-type strain, the isogenic *slm1*Δ mutant strain was supersensitive to myriocin. The growth of the *slm1*Δ mutant was already severely delayed at myriocin concentrations as low as 0.25 μg/ml and was completely inhibited at 0.5 μg/ml (Fig. 2A). In contrast, the growth of the wild-type strain was normal under these conditions (Fig. 2A and data not shown). Deletion of *SLM2* also conferred enhanced sensitivity to myriocin, but perhaps due to the much lower abundance of the Slm2 protein (3), the effect was far less pronounced (Fig. 2A).

To determine whether myriocin-mediated growth inhibition is a direct consequence of sphingolipid depletion, we asked whether exogenous addition of PHS could rescue the myriocin supersensitivity of *slm1*Δ cells. PHS has been shown to reverse

myriocin-mediated growth inhibition (53) and, as shown in Fig. 2B, addition of exogenous PHS to growth medium containing myriocin also restored growth to *slm1*Δ mutant cells. Thus, Slm1 is required for growth when de novo sphingolipid biosynthesis is compromised, suggesting that Slm proteins function in a process that is modulated by intracellular sphingolipid concentration.

Genetic interaction between *slm1*Δ and mutants in the sphingolipid biosynthesis pathway. To further establish a functional relationship between Slm proteins and sphingolipids, we examined whether the combination of an *slm1*Δ mutation with mutations in sphingolipid biosynthetic genes results in synergistic effects and leads to synthetic sickness or lethality. To do this, heterozygous diploids were generated by crossing an *SLM1* deletion mutant strain with a panel of mutants with isogenic deletion mutations that block various nonessential steps in the sphingolipid biosynthesis pathway (Fig. 1). The resulting diploid strains were then sporulated, and tetrads were dissected, allowed to germinate at 30°C on rich medium, and analyzed for segregation of genetic markers.

Viable doubly mutant progeny were recovered in all crosses tested, demonstrating that none of the double-mutant combinations is synthetically lethal. However, *slm1*Δ conferred temperature-sensitive growth when combined with deletion mutations in three genes: *FEN1*, whose product regulates fatty acid elongation (43) (Fig. 1); *LCB4*, which encodes the major sphingoid base kinase that phosphorylates DHS and PHS to DHS-1P and PHS-1P (42) (Fig. 1); and *CSG2*, which is required for the mannosylation of IPC to form the complex sphingolipid MIPC (56, 61) (Fig. 1). Accordingly, compared to results for single mutant and wild-type strains, colony formation and growth of *slm1*Δ *csg2*Δ, *slm1*Δ *fen*Δ*1*, and *slm1*Δ *lcb4*Δ double mutant strains were severely compromised at 38°C but were not affected at 26°C (Fig. 3A). Attempts to test for synthetic lethality between *slm2*Δ and either *csg2*Δ, *fen1*Δ, or *lcb4*Δ were unsuccessful, because the diploid strains failed to sporulate (data not shown). Nevertheless, we conclude that loss of Slm1 confers temperature-sensitive growth when combined with mutations that affect sphingolipid biosynthesis (3, 20). Because de novo sphingolipid biosynthesis is required for heat stress resistance (19, 32, 58), our findings suggest that Slm1 and sphingolipids play a common role required for survival under heat stress conditions.

Loss of sphingolipid synthesis results in defects in actin cytoskeletal organization (23, 60). Notably, these defects are similar to those previously reported for yeast mutants lacking Slm function (3, 20), suggesting that sphingolipids and Slm proteins may cooperate to regulate proper actin polarization. To investigate this hypothesis, we visualized actin in *slm1*Δ *csg2*Δ, *slm1*Δ *fen1*Δ, and *slm1*Δ *lcb4*Δ double-mutant cells by fluorescence microscopy using Alexa594-conjugated phalloidin. When shifted to 38°C for 2 h, all double-mutant cells exhibited severe actin cytoskeletal defects. Actin patches were completely depolarized and distributed evenly between mother and daughter cells, and actin cables were either faint or completely absent (Fig. 3B). In contrast, actin cytoskeletal organization in the single-mutant cells was similar to that in the wild type, with actin cables traversing from mother to bud and actin patches polarized toward the bud tip (Fig. 3B). Consistent with the temperature-sensitive growth of the double mutants, actin polarization defects were also temperature dependent and observed only at 38°C, not at 26°C (data not shown). Taken together, these data indicate that Slm proteins and sphingolipids play a redundant role in promoting cell growth and proper actin polarization during heat stress.

Depletion of cellular sphingolipid levels only weakly affects Slm1 plasma membrane association. Sphingolipid biosynthesis is required for plasma membrane localization of lipid raft-associated proteins (4, 40). Because Slm1 and Slm2 showed partially overlapping localization with multiple lipid raft-associated proteins, including Pma1, Can1, and Sur7 (20) (see Fig. S1 in the supplemental material), this raised the question of whether sphingolipid synthesis was also required for Slm1 and Slm2 plasma membrane association (3, 20). To investigate this possibility, we examined the subcellular localization of an Slm1-GFP fusion protein, expressed under the control of its endogenous promoter, in cells treated with various concentrations of myriocin. These experiments showed that Slm1-GFP localization to punctate foci at the plasma membrane was not noticeably affected when cells were incubated at 26°C in the presence of up to 2 μg/ml myriocin (data not shown). A moderate decrease in plasma membrane Slm1-GFP signal was observed when cells were exposed to toxic concentrations of myriocin (2 μg/ml) in combination with mild heat shock treatment (3 h at 38°C; data not shown), suggesting that sphingolipids, in part, are required for Slm targeting to the plasma membrane under heat stress conditions. However, even under these conditions, a significant portion of GFP-Slm1 was still observed in punctate foci at the plasma membrane (data not shown). In addition, HA-Slm1 localized normally to the plasma membrane in the temperature-sensitive *lcb1-100* mutant (data not shown), which is defective for sphingolipid biosynthesis (26). Taken together, our data suggest that sphingolipids are dispensable for Slm plasma membrane association under regular growth conditions and only moderately affect Slm1 plasma membrane targeting under heat stress conditions, raising the possibility that sphingolipids modulate Slm function by an additional mechanism.

Sphingolipids modulate Slm1 and Slm2 phosphorylation in response to heat stress. Slm1 and Slm2 are phosphoproteins in vivo, and previous studies have demonstrated that Slm proteins are dephosphorylated immediately following heat shock and become rephosphorylated during the recovery period (3). Because de novo sphingolipid synthesis is transiently upregulated during heat stress, we wished to determine whether sphingolipids affect Slm phosphorylation. To this end, strains containing chromosomally integrated TAP-tagged Slm1 and Slm2 were grown to mid-logarithmic phase in YPD medium at 26°C, separated into aliquots, and either shifted to 38°C for various periods or left at 26°C. Cell extracts were then prepared, and TAP-tagged Slm1 and Slm2 were purified by IgG-Sepharose affinity purification, separated by SDS-PAGE, and detected by immunoblotting using anti-TAP antibodies or antibodies that specifically recognize phosphoserine (Q5) and phosphothreonine (Q7) residues.

As shown in Fig. 4A, Slm1 produced prominent Q5/Q7-immunoreactive bands of the expected molecular weight for Slm1-TAP, suggesting that Slm1 is phosphorylated on both serine and threonine residues. The intensity of Q5 and Q7

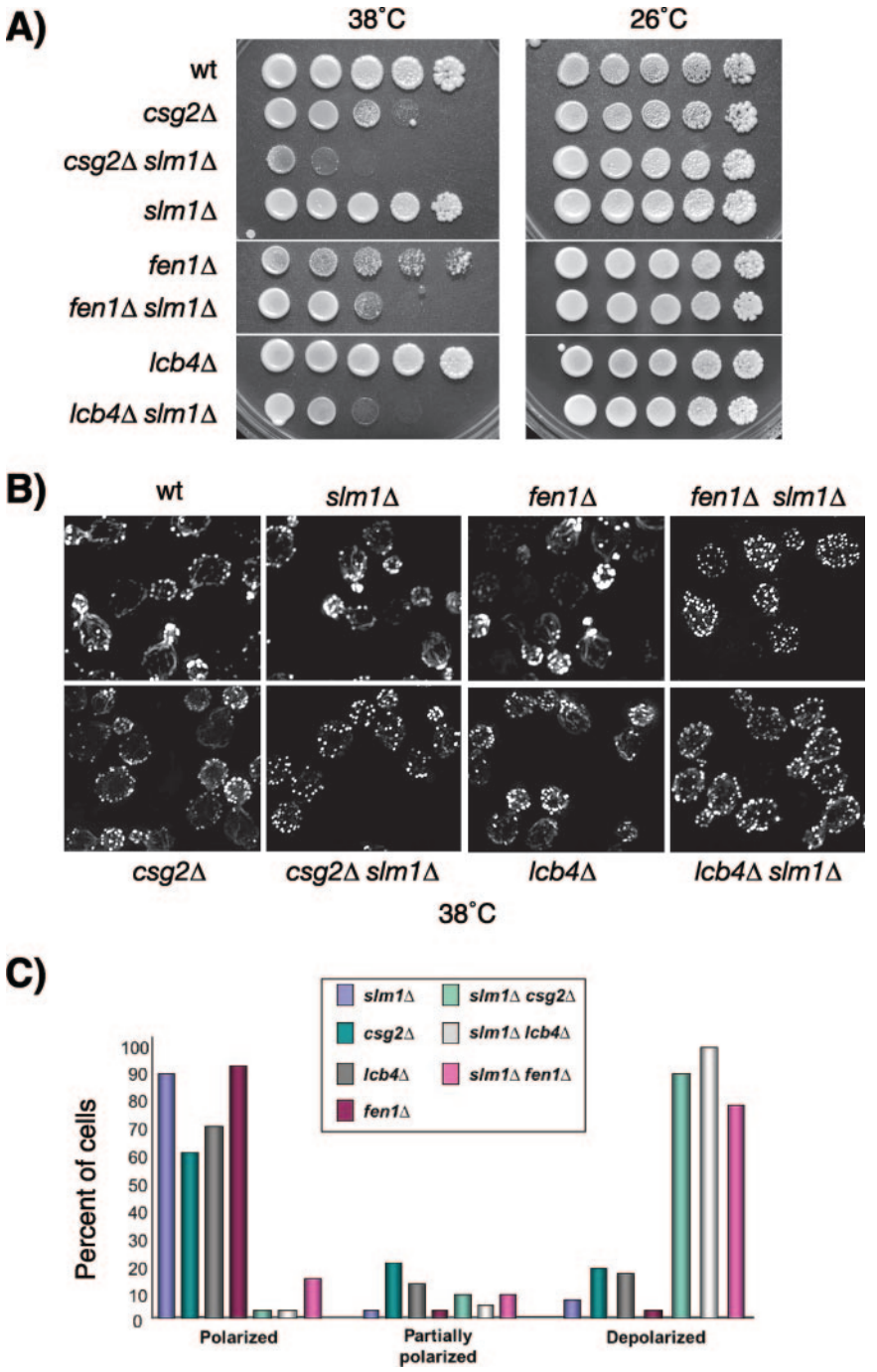

FIG. 3. Synthetic genetic interactions between *slm1*Δ mutants and mutants with mutations in the sphingolipid biosynthesis pathway. (A) Serial dilutions of isogenic wild-type, *slm1*Δ, *csg2*Δ, *fen1*Δ, and *lcb4*Δ single-mutant, and *slm1*Δ *csg2*Δ, *slm1*Δ *fen1*Δ, and *slm1*Δ *lcb4*Δ double-mutant yeast cultures were spotted on YPD plates. Plates were incubated at 26°C and 38°C and photographed after 3 days. (B) Exponentially growing wild-type, *slm1*Δ, *csg2*Δ, *fen1*Δ, and *lcb4*Δ single-mutant and *slm1*Δ *csg2*Δ, *slm1*Δ *fen1*Δ, and *slm1*Δ *lcb4*Δ double-mutant yeast cultures grown at 26°C were shifted to 38°C for 2 h. Cells were fixed and stained with Alexa594-phalloidin to visualize the actin cytoskeleton. (C) Small- to medium-budded cells from panel B were scored for their actin polarization state. Cells were classified as having an actin cytoskeleton that was polarized (containing cables and polarized actin patches), partially polarized (containing cables and partially polarized patches), or depolarized (containing no cables and depolarized patches). One hundred cells per sample were counted.

signals immediately following heat shock (5 to 10 min) either did not change or weakly decreased (Q5) (Fig. 4C). However, a significant increase in Q5 and Q7 signal intensity was observed later during heat shock, suggesting that Slm1 phosphorylation on serine and threonine residues is stimulated during the recovery period (Fig. 4A and C). Slm2 also produced Q5/Q7-immunoreactive bands (Fig. 4B). However, due to the approximately 10-fold-lower abundance of Slm2 protein in

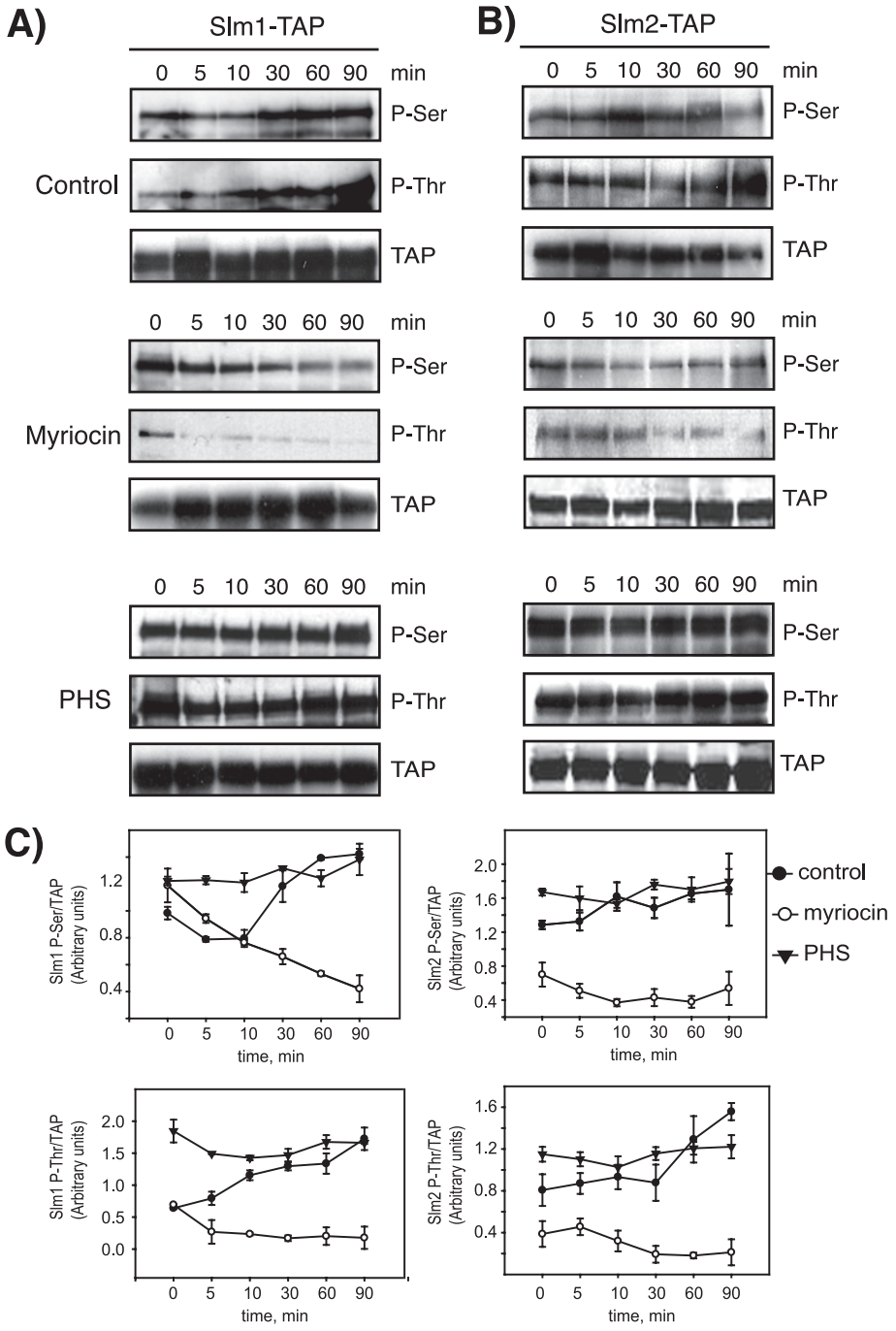

FIG. 4. Slm1 and Slm2 phosphorylation in response to heat stress is dependent on sphingolipid synthesis. Western blot analysis of phosphorylated Slm1 (A) and Slm2 (B) proteins is shown. Cells expressing Slm1-TAP and Slm2-TAP were grown to mid-logarithmic phase in YPD medium at 26°C; aliquots of cells were then treated with vehicle alone (dimethyl sulfoxide), myriocin (2 μg/ml), or exogenous PHS (10 μM) for 30 min at RT and heat shock-shifted to 38°C for the indicated times. Cell extracts were prepared and subjected to TAP purification using IgG-Sepharose beads. Bound proteins were eluted with SDS-PAGE buffer, separated by SDS-PAGE, and immunoblotted with antibodies directed against phosphoserine (Q5) and phosphothreonine (Q7). Note that Slm2 Western blots were exposed to ECL reagents eight times longer than Slm1. (C) Quantitation of kinetics of Slm1 and Slm2 phosphorylation in response to heat stress in the presence or absence of drugs. Densitometric measurements of Western blots in panels A and B were made with the Image Gauge 4.0 program. Q5 and Q7 signals were normalized to the TAP signal for each time point. Results from two independent experiments are shown.

wild-type cell extracts, the Q5/Q7 signals were weak and difficult to quantitate reproducibly (Fig. 4B and C; note that exposure times of Western blots shown are eightfold longer than with Slm1), and our subsequent analysis thus mainly focused on Slm1. Nevertheless Slm2 phosphorylation modestly increased during heat shock, as judged by increases in Q5 and Q7 signal intensity (Fig. 4B and C). Taken together, our data are in good agreement with earlier studies (3) and demonstrate

that Slm1 and Slm2 phosphorylation on serine and threonine residues is stimulated in response to heat shock.

To examine whether the phosphorylation status of Slm1 and Slm2 is modulated by sphingolipids, cells were preincubated with myriocin (2 μg/ml final concentration) for 30 min at RT to block cellular sphingolipid synthesis and were then shifted to 38°C. Protein extracts were prepared after various periods, and Slm1-TAP and Slm2-TAP were isolated, separated by SDS-PAGE, and probed with anti-TAP, -Q5, and -Q7 antibodies. Myriocin treatment completely abolished the heat-induced increase in Q5- and Q7-immunoreactive bands and, over time, decreased Q5 and Q7 signals below basal levels (Fig. 4), indicating that de novo sphingolipid synthesis is essential for stimulating Slm1 and Slm2 phosphorylation during heat stress. Consistent with a role for sphingolipids in promoting Slm phosphorylation, we found that pretreatment of cells with exogenous PHS (10 μM) for 30 min before heat shock significantly increased basal levels of Slm1 and moderately increased Slm2 phosphorylation compared to control cells, as judged by the intensity of Q5 and Q7 signals (Fig. 4). PHS also enhanced phosphorylation of Slm1 during early periods of heat shock. Together, our data argue that the stimulation of Slm phosphorylation on serine and threonine residues observed in response to heat stress is mediated by an increase in de novo sphingolipid synthesis.

Calcineurin dephosphorylates Slm proteins during heat stress. Genome-wide two-hybrid studies demonstrated that Slm2 interacts with Cna1 and Cna2 (31, 57), the catalytic subunits of the Ca^{2+}/calmodulin-dependent serine/threonine protein phosphatase calcineurin (13). These findings suggested that Slm2, and possibly Slm1, may be a substrate of calcineurin and dephosphorylated in vivo. In support of such a hypothesis, potential calcineurin binding sites that fit the consensus binding motif PxIxIT/Q (12, 38) are present in the extreme C-terminal regions of both Slm1 (amino acids 668 to 682) and Slm2 (amino acids 636 to 649) (Fig. 5A).

To confirm the two-hybrid interaction between Slm2 and calcineurin subunits, we performed in vitro pull-down assays using recombinant purified His_6-tagged Slm1 and Slm2 fusion proteins and ^{35}S-labeled Cna1 generated by a coupled transcription/translation reaction. As shown in Fig. 5B, Cna1 was readily recovered on agarose beads containing bound His_6-Slm1 and His_6-Slm2 but not on resin alone. In contrast, Slm1 and Slm2 mutants lacking the potential C-terminal calcineurin-binding domain failed to retain Cna1 (Fig. 5B). Thus, Slm1 and Slm2 directly associate with Cna1, suggesting that Slm1 and Slm2 are novel targets of calcineurin.

To explore whether Slm1 and Slm2 are regulated by calcineurin in vivo, we monitored Slm phosphorylation during heat stress under conditions that activate or inactivate calcineurin. Birchwood and colleagues previously showed that heat shock or exogenous PHS stimulates Ca^{2+} influx via the plasma membrane Cch1 channel, resulting in accumulation of intracellular Ca^{2+} and activation of calcineurin (7). They further demonstrated that calcineurin activation can be stimulated by high extracellular Ca^{2+} concentrations and blocked by the non-membrane-permeative Ca^{2+} chelator BAPTA. To determine whether Slm proteins are substrates for calcineurin during heat stress, we monitored Slm1 and Slm2 phosphorylation in yeast cells pretreated with $CaCl_2$ (100 mM) or BAPTA (10 μM) for 30 min prior to heat shock. Compared to control-treated yeast cells, Q5/Q7 immunoreactive Slm1 (Fig. 5C and D) and Slm2 (data not shown) signals were significantly decreased at all time points in extracts derived from cells challenged with high concentrations of extracellular Ca^{2+}. Conversely, blocking Ca^{2+} influx by pretreatment of yeast cells with BAPTA significantly enhanced Slm1 and Slm2 phosphorylation (Fig. 5C and D [Slm1] and data not shown [Slm2]), as judged by the increase in Q5 and Q7 signal intensities. Importantly, BAPTA significantly stimulated basal phosphorylation and also enhanced Slm phosphorylation immediately following heat shock. Taken together, our results demonstrate that Slm phosphorylation is downregulated in response to Ca^{2+} influx, possibly by activation of a Ca^{2+}-activated phosphatase that counteracts heat-induced phosphorylation.

To determine whether Slm dephosphorylation is mediated by calcineurin, we pretreated cells with the immunosuppressive drug FK506, which is a specific inhibitor of calcineurin (36). FK506 treatment caused a noticeable increase in basal Slm1 phosphorylation on serine and threonine residues and also enhanced phosphorylation during the early phases of heat shock compared to control-treated cells (Fig. 5C and D) but did not affect maximal phosphorylation levels. To determine whether Slm1 is an in vivo substrate of calcineurin, we compared serine and threonine phosphorylation levels of wild-type Slm1 and the $Slm1_{\Delta CN}$ mutant, which lacks the C-terminal calcineurin-binding site. Both proteins were expressed in wild-type cells as N-terminal TAP fusion proteins from the galactose-inducible *GAL1* promoter and were then purified and analyzed by Western blotting using Q5 and Q7 antibodies. As shown in Fig. 5E and F, the serine and threonine phosphorylation of $Slm1_{\Delta CN}$ was increased compared to that of wild-type Slm1 in the absence of heat stress stimulation and remained increased over the wild-type level during early phases of heat treatment. These data demonstrate that Slm proteins are substrates of the protein phosphatase calcineurin and suggest that calcineurin counteracts Slm phosphorylation when cells are grown at physiological temperatures and immediately following heat shock. Collectively, our data argue that Slm proteins are subject to both positive and negative control by kinases and phosphatases in response to cellular stress.

To better understand the physiological role of calcineurin and sphingolipid-mediated regulation of Slm, we next investigated whether the temperature-sensitive growth of an *slm1-ts slm2*Δ mutant strain (JK515) could be rescued by addition of FK506 or PHS to the growth medium. As shown in Fig. 6, FK506 and PHS, when added together, were able to partially restore growth at the nonpermissive temperature, whereas little effect was observed when FK506 and PHS were added alone. One interpretation of these results is that calcineurin and sphingolipids antagonistically regulate Slms with calcineurin-mediated dephosphorylation-inhibiting and PHS-stimulating Slm functions. Thus, by simultaneously providing the stimulatory signal and blocking calcineurin-mediated inhibition, Slm activity may be maximally enhanced. In agreement with such a hypothesis, we found that growth and actin defects of *slm1*Δ *csg2*Δ, *slm1*Δ *fen1*Δ, and *slm1*Δ *lcb4*Δ double mutants at 38°C could be significantly suppressed by the combined addition of PHS and FK506 to the growth medium, whereas

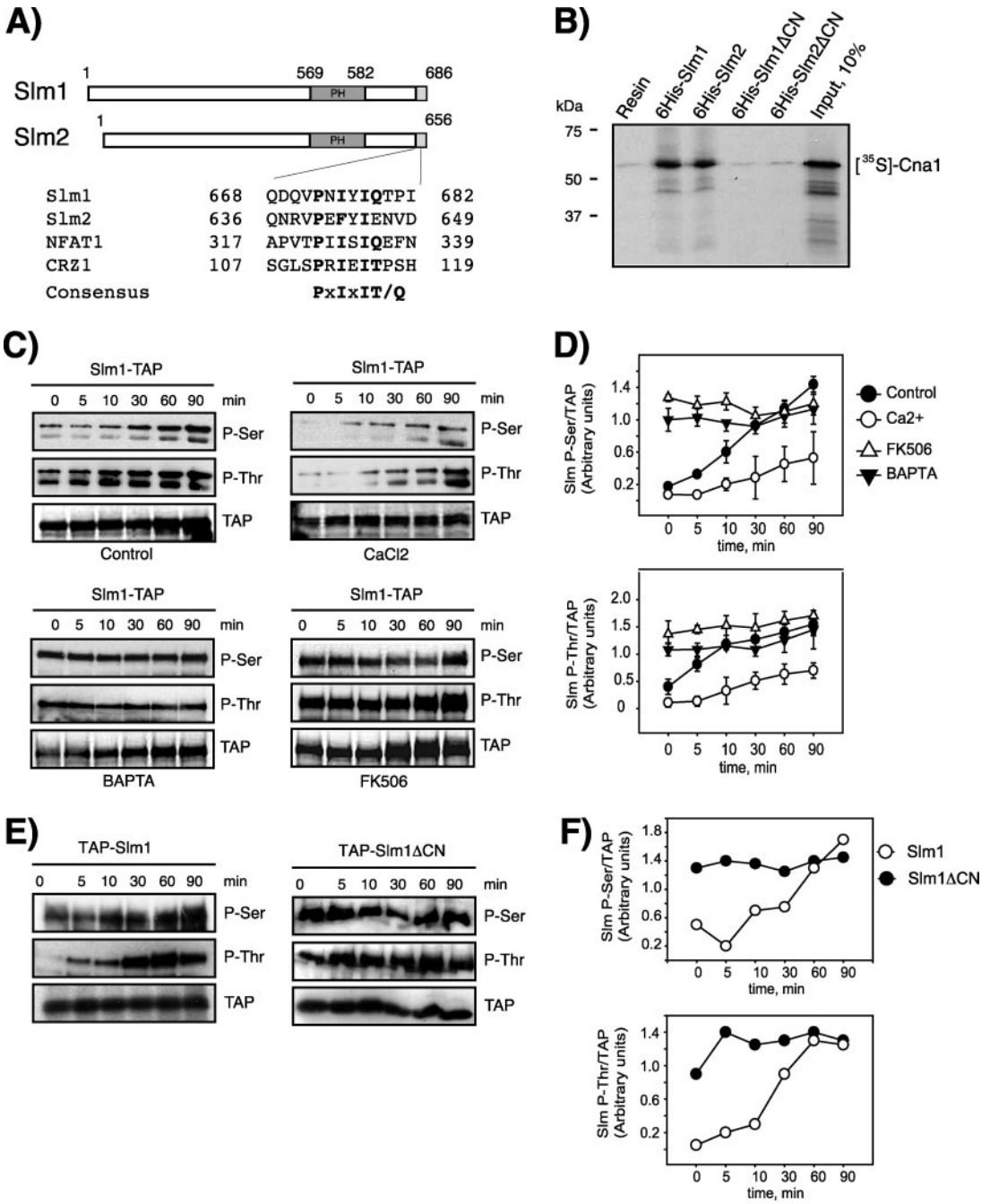

FIG. 5. The Ca^{2+}/calmodulin-dependent protein phosphatase calcineurin dephosphorylates Slm1. (A) Sequence alignment of Slm1 and Slm2 with known calcineurin binding sites. The consensus calcineurin-binding motif is given below the sequence alignment. (B) In vitro-transcribed and -translated ^{35}S-labeled Cna1 was incubated with beads alone or with beads containing bound recombinant His_6-Slm1 or His_6-Slm2 proteins or Slm mutant variants lacking the calcineurin-binding motif. Bound ^{35}S-labeled proteins that remained after washing were analyzed by SDS-PAGE and autoradiography. The molecular masses of protein markers are indicated on the left. (C) Cells expressing Slm1-TAP were grown to mid-logarithmic phase in YPD medium at 26°C, divided into aliquots, and treated for 30 min at RT with vehicle alone (dimethyl sulfoxide), 100 mM $CaCl_2$, 10 μM BAPTA, or FK506 (2 μg/ml). Cells were shifted to 38°C for the indicated times, and cell extracts were prepared and subjected to TAP purification using IgG-Sepharose beads. Bound proteins were separated by SDS-PAGE and immunoblotted with antibodies directed against phosphoserine (Q5) and phosphothreonine (Q7). (D) Densitometric analysis of phosphorylation levels of Slm1-TAP from panel C. Western blots were digitized with the Image Gauge 4.0 program, and the levels of phosphorylation were normalized to the TAP signal at each time point. (E) Wild-type cells expressing Slm1-TAP or the $Slm1_{\Delta CN}$-TAP mutant from a low-copy-number vector under the control of the Gal1 promoter were grown at 26°C in the presence of galactose for 2.5 h to induce expression of the TAP fusion protein. Glucose was then added to shut off expression, and incubation was continued for 30 min at 26°C. Cells were then heat shocked at 38°C for the indicated times. Extracts were prepared and analyzed as described for panel C. (F) Densitometric analysis of phosphorylation levels of Slm1-TAP from panel E. Results from two independent experiments are shown.

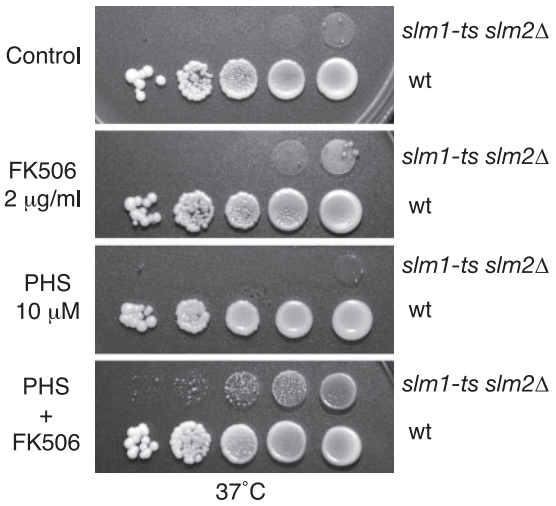

FIG. 6. FK506 and exogenous PHS rescue the lethality of *slm1-ts slm2*Δ mutant cells. Serial dilutions of isogenic wild type, and *slm1-ts slm2*Δ mutant yeast cultures were spotted on YPD plates either containing drug vehicle (Tween 20-ethanol [Control]) or supplemented with FK506 (2 μg/ml), PHS (10 μM), or both. Plates were incubated at 37°C and photographed after 3 days.

addition of either reagent alone was less effective (see Fig. S2 in the supplemental material).

Slm1 phosphorylation involves the sphingolipid-activated kinases Pkh1 and Pkh2. Previous studies identified the functionally redundant protein kinases Pkh1 and Pkh2 as effectors of sphingolipid signaling and demonstrated that the two kinases are directly activated in vitro by nanomolar concentrations of sphingoid bases (22, 29). To determine whether Slm1 phosphorylation is dependent on Pkh1/2, we expressed HA-tagged *SLM1* under the control of the *GAL1* promoter from a low-copy-number vector in wild-type and temperature-sensitive *pkh1-ts pkh2*Δ mutant cells. HA-Slm1 synthesis was induced at 26°C for 2 h in the presence of galactose, and then glucose was added to shut off further expression. After a 30-min incubation, cells were shifted to the nonpermissive temperature (38°C), and Slm1 phosphorylation was examined using Q5 and Q7 phosphospecific antibodies. As expected, there was a pronounced increase in phosphoserine and phosphothreonine levels of Slm1 during the course of heat shock treatment of wild-type cells (Fig. 7). In contrast, *pkh1-ts pkh2*Δ cells showed reduced basal and heat-induced phosphorylation on serine and threonine as determined by the levels of intensity of the Q5 and Q7 signals (Fig. 7). While there was an initial weak increase in Q5 and Q7 signals following shift to 38°C, likely due to residual Pkh activity, the increase in Q5 and Q7 signals typically observed after longer incubation at 38°C (30 to 90 min) was abrogated in *pkh1-ts pkh2*Δ cells (Fig. 7). These results suggest that Slm1 phosphorylation on serine and threonine residues is at least partially regulated by the sphingoid base-dependent Pkh signaling cascade during heat stress and that the Pkh kinases may be upstream regulators of the Slm pathway.

To determine whether Pkh kinases directly phosphorylate Slm proteins, we expressed Pkh1 as a His_6 fusion protein in *E. coli*, purified the recombinant protein, and tested whether it could phosphorylate recombinant GST-Slm1 or GST-Slm2 in an in vitro kinase assay as described previously (37). However, while efficient Pkh1 autophosphorylation was observed, no phosphorylation of Slm1 or Slm2 was detected (data not shown). Thus, Slm1 and Slm2 phosphorylation is indirectly modulated by Pkh kinases.

Pkh1 and Pkh2 phosphorylate and activate a pair of redundant protein kinases termed Ypk1 and Ypk2 that are essential for growth and the regulation of cell wall integrity and actin cytoskeleton polarization (9, 46, 47). PHS can directly stimulate these kinases or activate them indirectly via Pkh1/2 (37). To determine whether Slm1 phosphorylation involves Ypk kinases, we expressed *HA-SLM1* in the temperature-sensitive *ypk1-ts ypk2* mutant strain and measured phospho-Slm1 levels during heat shock treatment. In contrast to cells lacking Pkh activity, yeast mutants defective in Ypk1/2 showed no apparent defect in the rate of heat-induced Slm phosphorylation (Fig. 7). Heat-induced increases in Q5/Q7 signals were also observed in cells containing a temperature-sensitive mutation in the Tor2 kinase (Fig. 7), which was previously shown to phosphorylate Slm1 in vitro and in vivo (3, 20). Thus, heat stress-induced phosphorylation of Slm1, at least as visualized by Q5 and Q7 antibodies, appears to involve Pkh, but not Ypk or Tor2 kinases.

Phosphorylation of Ser659 is essential for Slm1 function under heat stress conditions. To gain insight into how Slm activity is affected by phosphorylation, we next undertook to identify phosphorylation sites in Slm1. Slm1-TAP protein expressed under control of its endogenous promoter was purified from cells incubated at 38°C for 90 min to stimulate Slm1 phosphorylation. Purified Slm1-TAP was then resolved by SDS-PAGE and visualized by staining with Coomassie brilliant blue. The band corresponding to Slm1-TAP was extracted from the gel, subjected to tryptic proteolysis, and analyzed by mass spectrometry (see Materials and Methods). Analysis of the MS/MS spectra identified 22 predicted Slm1 tryptic peptides containing a common phosphoserine site, T_{653}NTSMSS(p)LPDT, with Xcorr scores of >4.0 (data not shown), suggesting that this residue represents a major site of phosphorylation. No other candidate phosphorylation sites were detected. Ser_{659} is conserved in Slm2 (corresponding to Ser_{626}) and immediately precedes the calcineurin binding site (amino acids 668 to 682).

To probe the potential function of Ser_{659} phosphorylation, we generated a phosphorylation site-defective Slm1 mutant ($Slm1_{S659A}$) in which Ser_{659} was replaced with Ala. To confirm that this single amino acid change affects heat-induced phosphorylation, we first expressed the $Slm1_{S659A}$ mutant as an HA-tagged protein in wild-type cells, subjected cells to heat shock treatment, and analyzed the purified HA-$Slm1_{S659A}$ protein for phosphorylation using Q5 and Q7 antibodies. Immunoblotting with anti-TAP and Q7 antiserum revealed similar levels of TAP immunoreactivity in the $Slm1_{S659A}$ mutant as in the corresponding wild-type protein, and in both cases, the expected increase in Q7 signals in response to heat shock treatment was observed (Fig. 8A). In contrast, immunoblotting with Q5 antiserum revealed only basal levels of Slm1 phosphorylation, whereas the typical heat-induced increase in Q5 signal was completely abrogated in the $Slm1_{S659A}$ mutant (Fig. 8A). Together, these experiments confirm that Ser_{659} is indeed the

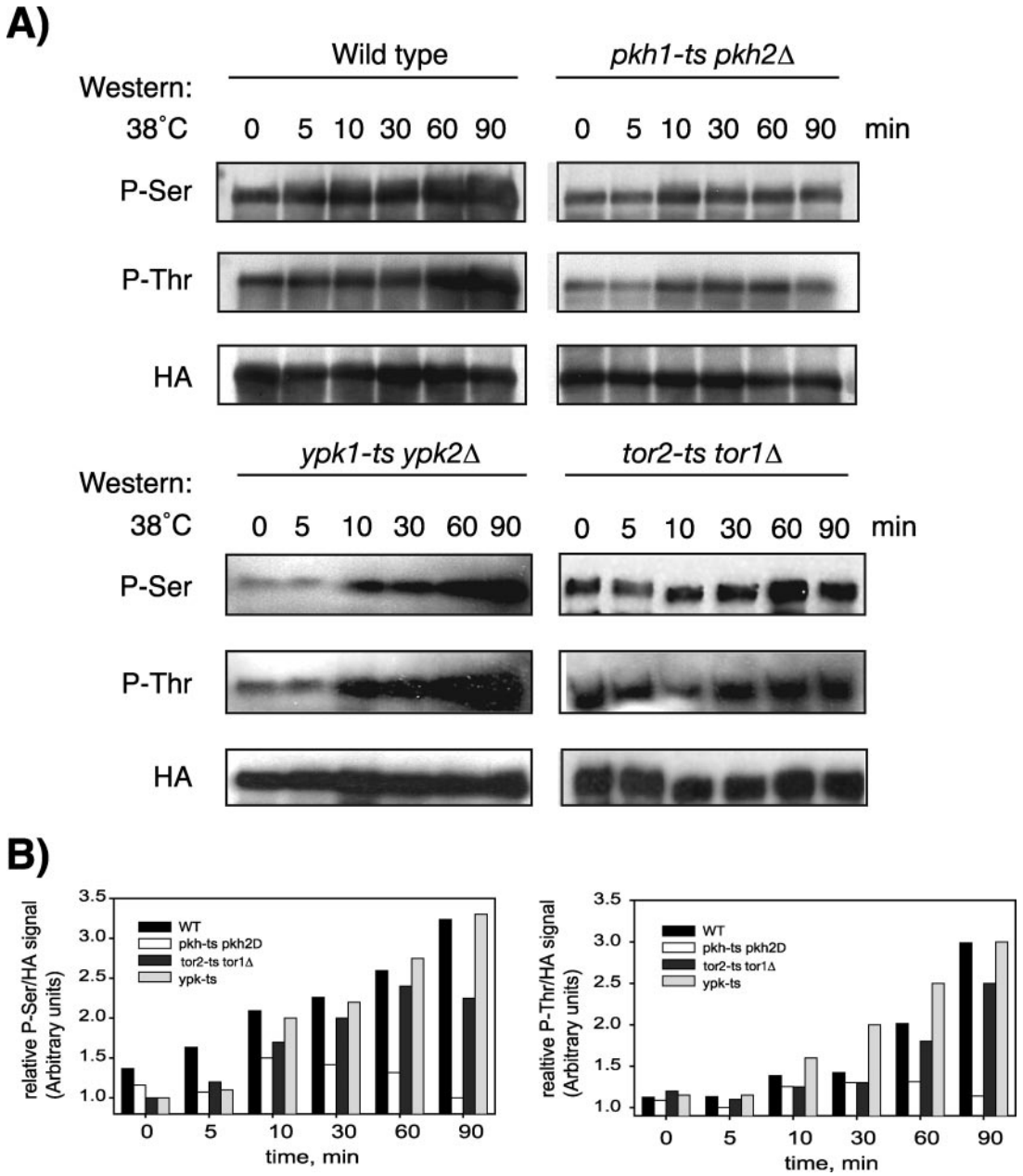

FIG. 7. Slm1 phosphorylation is dependent on the sphingolipid-activated kinases Pkh1/2 and Pkh2 but is independent of Ypk1/2 and Tor2. (A) Exponentially growing wild-type or temperature-sensitive *pkh1-ts pkh2*Δ, *ypk1-ts ypk2*Δ (strain YPT40), or *tor1*Δ *tor2-ts* (strain SH121) mutant cells that contain HA-Slm1 under the control of a galactose-inducible promoter were grown at 26°C in the presence of galactose for 2.5 h to induce expression of HA-Slm1. Glucose was then added to shut off expression, and incubation was continued for 30 min at 26°C. Cells were then heat shocked at 38°C for the indicated times. Extracts were prepared and subjected to affinity purification on anti-HA-Sepharose beads. Bound proteins were separated by SDS-PAGE and immunoblotted with antibodies directed against phosphoserine (Q5), phosphothreonine (Q7), and HA. (B) Western blot densitometric analysis of phosphorylation levels of HA-Slm1. Blots were digitized with the Image Gauge 4.0 program, and the levels of phosphorylation were normalized to the HA signal.

major serine residue phosphorylated during the heat stress response and that mutagenesis of this site specifically affects serine but not threonine phosphorylation during heat treatment.

To test whether phosphorylation at Ser_{659} is required for Slm1 activity, we employed a plasmid-shuffling assay. An *slm1*Δ *slm2*Δ double mutant strain carrying an *SLM1 URA3* plasmid (strain JK520) was transformed with a second plasmid containing *LEU2* as a marker and containing either wild-type *SLM1* or the $SLM1_{S659A}$ variant. Transformants were then streaked on solid medium containing 5-fluoroorotic acid (5-FOA) to counterselect the *SLM1 URA3* plasmid. We found that *LEU2* plasmids (vector p425GPD) containing either wild-type *SLM1* or $SLM1_{S659A}$ could complement the lethality of *slm1*Δ *slm2*Δ null mutant cells on 5-FOA-containing medium at 30°C (Fig. 8C). However, only the *LEU2* plasmid containing wild-type

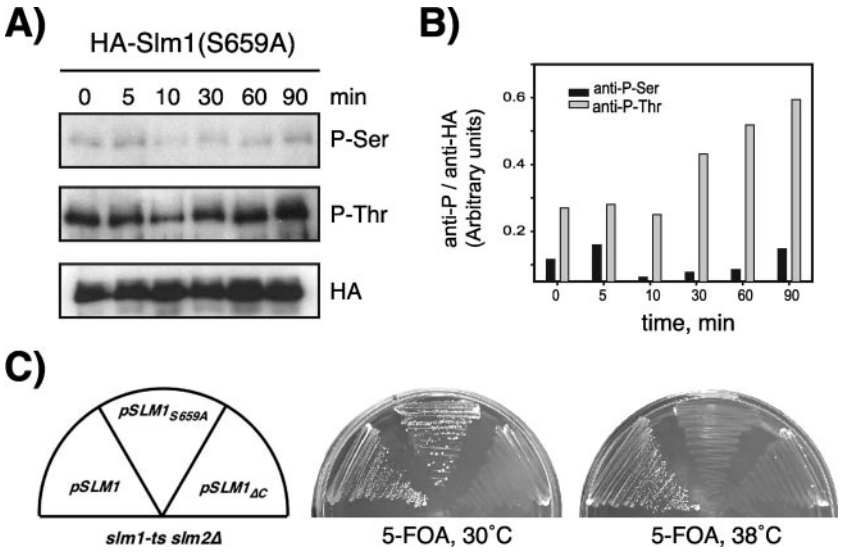

FIG. 8. Mutation of Ser659 abrogates Slm1 phosphorylation and Slm1-dependent survival under heat stress conditions. (A) Cells expressing HA-tagged $Slm1_{S659A}$ under control of the *GAL1* promoter were grown at 26°C in the presence of galactose for 2.5 h to induce expression of HA-Slm1. Glucose was then added to shut off expression, and incubation was continued for 30 min at 26°C. Cells were then heat shocked at 38°C for the indicated times. Extracts were prepared and subjected to affinity purification on anti-HA-Sepharose beads. Bound proteins were separated by SDS-PAGE and immunoblotted with antibodies directed against phosphoserine (Q5), phosphothreonine (Q7), and HA. (B) Densitometric analysis of phosphorylation levels of HA-$Slm1_{S659A}$ from panel A. (C) Growth of strain JK520 transformed with *LEU2* plasmids containing either wild-type *SLM1* or the $SLM1_{S659A}$ and $SLM1_{\Delta C}$ mutant variants at 30°C and 38°C on medium containing 5-FOA, which counterselects the *SLM1 URA3* plasmid.

SLM1 but not $SLM1_{S659A}$ was able to confer growth at 38°C (Fig. 8C). As expected, the *slm1*Δ *slm2*Δ double mutant transformed with a *LEU2* plasmid containing the inactive $SLM1_{\Delta C}$ mutant (20) was unable to grow on 5-FOA-containing medium at any temperature (Fig. 8C). We thus conclude that phosphorylation of Slm1 at Ser_{659} is dispensable for growth under normal growth conditions but is essential for survival under heat stress conditions.

***SLM1* overexpression partially rescues growth and actin defects of cells lacking Pkh function.** Because our biochemical data suggested that Pkh1/2 kinases are required for Slm1 phosphorylation, we wanted to explore what role Slm1 plays in Pkh1/2 signaling and whether phosphorylation at Ser_{659} confers enhanced Slm1 activity. To do this we mutated Ser_{659} in Slm1 to aspartate (yielding $Slm1_{S659D}$), because the introduction of an acidic charge often mimics phosphorylation. Galactose-induced expression of $SLM1_{S659D}$ from a low-copy-number plasmid (pAS25) rescued the temperature-sensitive growth of the *slm1-ts slm2*Δ mutant at 38°C, in contrast to $SLM1_{S659A}$ (data not shown), demonstrating that $Slm1_{S659D}$ is functional.

$SLM1_{S659D}$ or wild-type *SLM1* was then expressed in the *pkh1-ts pkh2*Δ mutant and tested for the ability to suppress the lethality of this mutant at the nonpermissive temperature. As expected, upon shifting to 38°C, growth was fully restored to *pkh1-ts pkh2*Δ mutant cells when *PKH1* was expressed from a low-copy-number plasmid (YCpG22-*PKH1*) under the control of the *GAL1* promoter (data not shown). In contrast, vector alone or expression of wild-type *SLM1* or $SLM1_{S659D}$ resulted in no or only very slight restoration of growth (data not shown). However, Pkh1 and Pkh2 are involved in the regulation of multiple essential cellular functions required for cell wall integrity and actin polarization. It was possible, then, that Slm proteins regulated only a subset of Pkh1-dependent essential functions. Indeed, microscopic examination of *pkh1-ts pkh2*Δ cells expressing *SLM1* revealed predominantly cell ghosts, suggesting that *SLM1* is unable to suppress the cell lysis defect of the *pkh1-ts pkh2*Δ mutant. To test whether *SLM1* suppresses the growth defect of *pkh1-ts pkh2*Δ cells in the presence of osmotic support, galactose plates were supplemented with 1 M sorbitol, and growth of transformants was assessed at 38°C. As shown in Fig. 9A, growth of the temperature-sensitive *pkh1-ts pkh2*Δ mutant transformed with empty vector was severely delayed at 38°C (Fig. 9A). Under these conditions, expression of $SLM1_{S659D}$ partially rescued the slow-growth defect of the *pkh1-ts pkh2*Δ mutant, although not as strongly as *PKH1* (Fig. 9A). Interestingly, expression of the $SLM1_{\Delta CN}$ mutant, which lacks the calcineurin-binding site, also suppressed the growth defect similarly to $SLM1_{S659D}$ and consistently better than wild-type *SLM1* (Fig. 9A).

Taken together, one reasonable explanation for our results is that the Pkh signaling cascade increases basal activity of Slm1 by promoting Slm phosphorylation and that this increase in activity is important for survival during heat stress and the repolarization of the actin cytoskeleton. If this is true, we would anticipate that the growth defect of the *pkh1-ts pkh2*Δ mutant is also suppressed by the exogenous addition of PHS and FK506, as this treatment is expected to result in increased Slm phosphorylation and enhanced Slm function. We found that this was indeed the case, as combined addition of PHS and FK506 to the growth medium significantly restored growth to *pkh1-ts pkh2*Δ mutant cells at the restrictive temperature of 34°C in the absence of osmotic stabilization, whereas addition of PHS or FK506 alone was less effective (see Fig. S3 in the supplemental material).

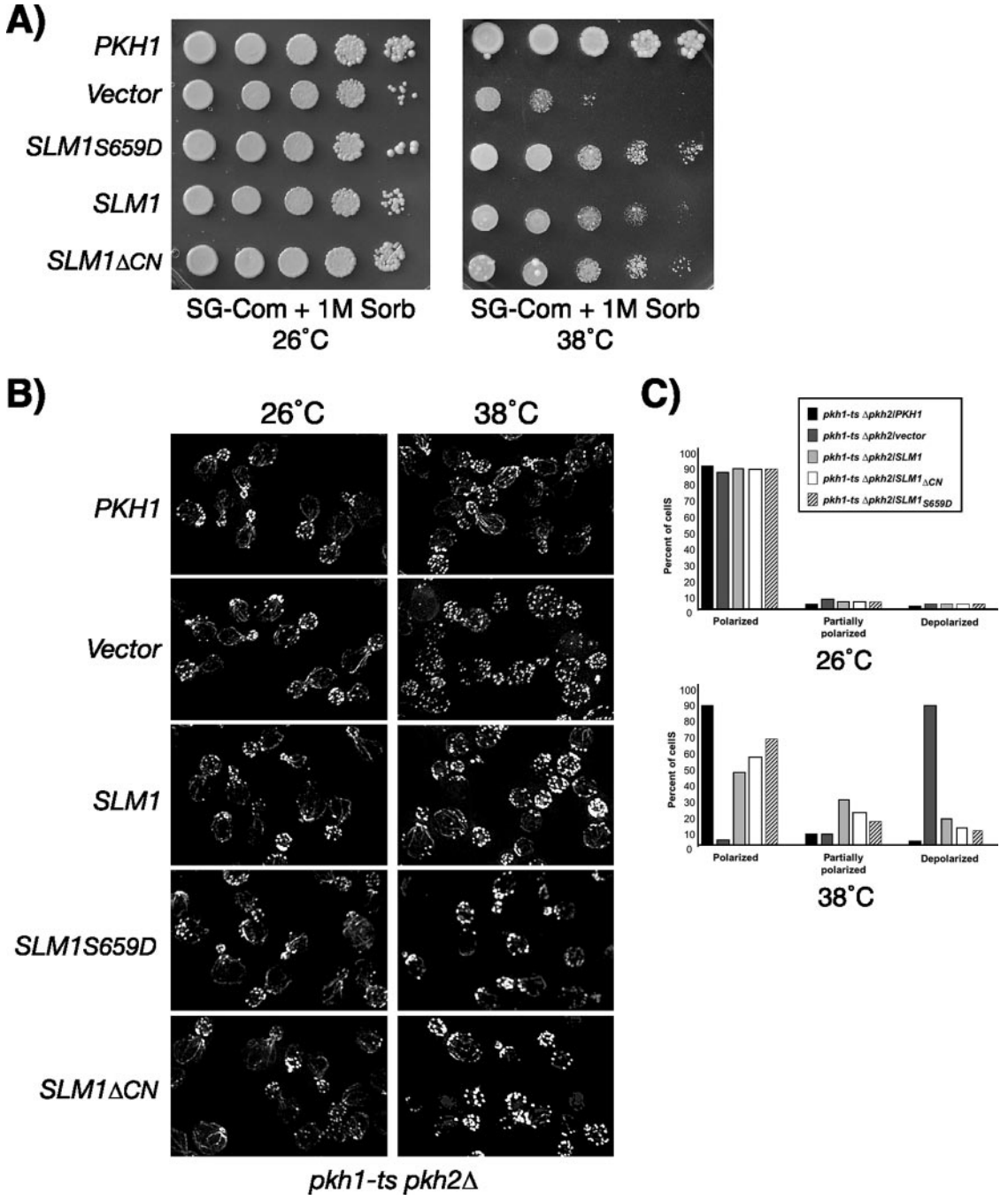

FIG. 9. *SLM1* overexpression partially corrects growth and actin polarization defects of *pkh1-ts pkh2*Δ mutant cells. (A) Vector alone or plasmids containing *PKH1*, *SLM1*, $SLM1_{S659D,}$ or $SLM1_{\Delta CN}$, under the control of the galactose-inducible *GAL1* promoter, were transformed into the temperature-sensitive *pkh1-ts pkh2*Δ mutant strain. Growth of transformants was tested on synthetic complete medium containing galactose as the carbon source and supplemented with 1 M sorbitol (SG, Sorb). Plates were incubated at the indicated temperatures and photographed after 3 to 4 days. (B) *pkh1-ts pkh2*Δ cells containing the indicated plasmids were grown at 26°C in medium supplemented with 1 M sorbitol and galactose. Cells were then shifted to 38°C for 2 h and fixed, and the actin cytoskeleton was visualized with Alexa594-phalloidin. (C) Small- to medium-budded *pkh1-ts pkh2*Δ mutants cells transformed with the indicated plasmids from panel B were scored for their actin polarization state. Cells were classified as having an actin cytoskeleton that was polarized (containing cables and polarized actin patches), partially polarized (containing cables and partially polarized patches), or depolarized (containing no cables and depolarized patches). One hundred fifty cells per sample were counted.

To further investigate the role of Slm1 in Pkh signaling, we assayed the ability of the Slm1 wild type and mutant variants to suppress the actin polarization defect of the *pkh1-ts pkh2*Δ mutant (46). To investigate whether Slm1 can restore proper actin polarization, *pkh1-ts pkh2*Δ mutant cells containing plasmids expressing *PKH1* or wild-type *SLM1* and mutant *SLM1* variants were grown at 26°C in medium osmotically stabilized with 1 M sorbitol and containing galactose to induce expres-

sion of *PKH1* and *SLM1*, respectively. Cells were then shifted to 38°C for 2 h and processed for visualization of the actin cytoskeleton. *pkh1-ts pkh2*Δ cells containing vector alone exhibited the expected random distribution of actin patches and lacked actin cables after incubation at 38°C for 2 h, even when grown in the presence of 1 M sorbitol (Fig. 9B and C). In contrast, *pkh1-ts pkh2*Δ cells expressing *PKH1* under the control of the *GAL1* promoter displayed the normal cell cycle-dependent polarized distribution of actin patches and cables (Fig. 9B and C). Actin polarization was also significantly restored in *pkh1-ts pkh2*Δ cells by expression of $SLM1_{S659D}$ and to a slightly lesser degree by expression of $SLM1_{\Delta CN}$ (Fig. 9B and C). Likewise, overexpression of wild-type *SLM1* rescued the actin polarization defects of *pkh1-ts pkh2*Δ cells, although less efficiently than expression of $SLM1_{S659D}$ and $SLM1_{\Delta CN}$ (Fig. 9B and C). Taken together, these data suggest that Slm proteins can provide a subset of essential Pkh-dependent functions involved in maintaining or restoring proper actin polarization.

Loss of Slm function results in mislocalization of the arginine permease Can1. Sphingolipids, in conjunction with sterols, are also involved in the transport of lipid raft-associated proteins to the plasma membrane. In particular, the targeting of plasma membrane H^+-ATPase Pma1 (4) and the arginine permease Can1 (40) to plasma membrane rafts was shown to be dependent on sphingolipid and ergosterol synthesis. Depletion of either of these raft lipids in *lcb1-100* or *erg24*Δ mutants abolished the transport of Pma1 and Can1 to the surface and resulted in their accumulation in intracellular compartments (3, 37).

To further explore a role of Slm1 and Slm2 in sphingolipid-dependent processes, we investigated whether trafficking of Pma1 and Can1 was affected in the *slm1-ts slm2*Δ mutant. The localization of Pma1 was examined by indirect immunofluorescence using anti-Pma1 antibodies. To monitor the localization of Can1, wild-type and *slm* mutant cells were transformed with a low-copy-number centromere-based plasmid (pCAN1-GFP) that produced Can1 as a GFP fusion protein, and the GFP signal was monitored in living cells. Pma1 and Can1 localization was compared in wild-type and *slm1-ts slm2*Δ cells either grown at the permissive temperature or shifted to 38°C for 2 h. Pma1 appeared to be similarly localized to the plasma membrane in wild-type and *slm1-ts slm2*Δ mutant cells (data not shown), suggesting that Slm proteins are not required for Pma1 trafficking. Can1-GFP, when expressed in wild-type cells, exclusively localized to the plasma membrane at both permissive and nonpermissive temperatures and exhibited the punctate fluorescence pattern characteristic of a lipid raft-associated protein (Fig. 10A). In contrast, Can1 targeting to the plasma membrane was partially defective at the permissive temperature (observed in 70% of cells) in *slm1-ts slm2*Δ cells and completely defective when cells were shifted to the nonpermissive temperature for 2 h (observed in 95% of cells). Under these conditions, Can1 accumulated in a perinuclear compartment and in areas adjacent to the plasma membrane (Fig. 10A). Consistent with previous reports (40), intracellular accumulation of Can1 was also observed in the *erg24*Δ mutant (100% of cells), which lacks the raft lipid ergosterol and is known to accumulate Can1 in the peripheral and perinuclear endoplasmic reticulum (ER) (40), and in the *lcb1-100* mutant, which accumulates Can1 in the ER and the Golgi (26°C, 93% of cells; 38°C, 100% of cells) (Fig. 10A). Expression of wild-type *SLM1* in *slm1-ts slm2*Δ cells significantly prevented the intracellular accumulation of Can1 at both permissive and nonpermissive temperatures, indicating that the defect in Can1 targeting is due to decreased Slm activity (Fig. 10B). The retention of Can1 in the ER could also be partially reversed by treatment of *slm1-ts slm2*Δ cells with PHS and FK506 (Fig. 10B).

Interestingly, mislocalization of Can1-GFP to perinuclear and peripheral ER compartments was also observed in the *pkh1-ts pkh2*Δ strain at both permissive (observed in 65% of cells) and nonpermissive (observed in 92% of cells) temperatures (Fig. 10A), raising the possibility that Pkh-dependent regulation of Slm proteins is required for Can1 trafficking. Consistent with such a hypothesis, overexpression of *SLM1* when combined with FK506 treatment of *pkh1-ts pkh2*Δ cells partially prevented the ER accumulation of Can1 (Fig. 10C).

Mutations that affect Can1 activity or its transport to the plasma membrane have been shown to confer increased resistance to the arginine analog canavanine, which is toxic to yeast (44). Thus, if loss of Slm function indeed affects Can1 trafficking to the plasma membrane, we would expect to observe a decrease in arginine uptake and a corresponding decrease in canavanine sensitivity. To examine this point, dilution series of wild-type and *slm1-ts slm2*Δ cultures were spotted on a plate containing 0.5 μg/ml canavanine and assayed for their ability to grow at 30°C. The parental wild-type strain W303 contains an endogenous mutation in the *CAN1* gene and showed growth at all dilutions on medium containing canavanine (Fig. 10D). However, transformation of W303 with the low-copy-number *GFP-CAN1* plasmid rendered cells canavanine sensitive (Fig. 10D). In contrast, the *slm1-ts slm2*Δ strain transformed with *GFP-CAN1* was resistant to canavanine, although not as strongly as the *lcb1-100* mutant (Fig. 10D). Because *slm1-ts slm2*Δ and *lcb1-100* mutants appear to accumulate Can1 in intracellular compartments, it is reasonable to assume that canavanine resistance is due to decreased canavanine uptake through Can1.

Because loss of Slm and Pkh function disrupts proper actin polarization, we next investigated whether the defect in Can1 trafficking observed in these mutants could be due to a defect in actin assembly. To do this, Can1-GFP localization was examined in wild-type cells treated with the drug latrunculin A, which rapidly depolymerizes actin. Consistent with previous reports, we found that latrunculin A did not cause Can1-GFP delocalization from the plasma membrane (Fig. 10E) (39). However, transport of newly synthesized Can1 from the ER to the plasma membrane was disrupted or delayed upon blocking actin assembly, because Can1-GFP signal accumulated in the ER and to a lesser degree on the Golgi over a treatment period of 120 min (Fig. 10E). Consistent with the hypothesis that Can1 transport is dependent on proper actin organization, intracellular retention of Can1 in the ER and the Golgi was also observed in temperature-sensitive *stt4*, *mss4*, and *tor2* mutants (data not shown), which exhibit actin defects at the nonpermissive temperature (2, 16, 48). Taken together, these data indicate that Slm proteins are required for efficient ER to plasma membrane trafficking of the lipid raft-associated permease Can1, possibly by promoting proper actin polarization.

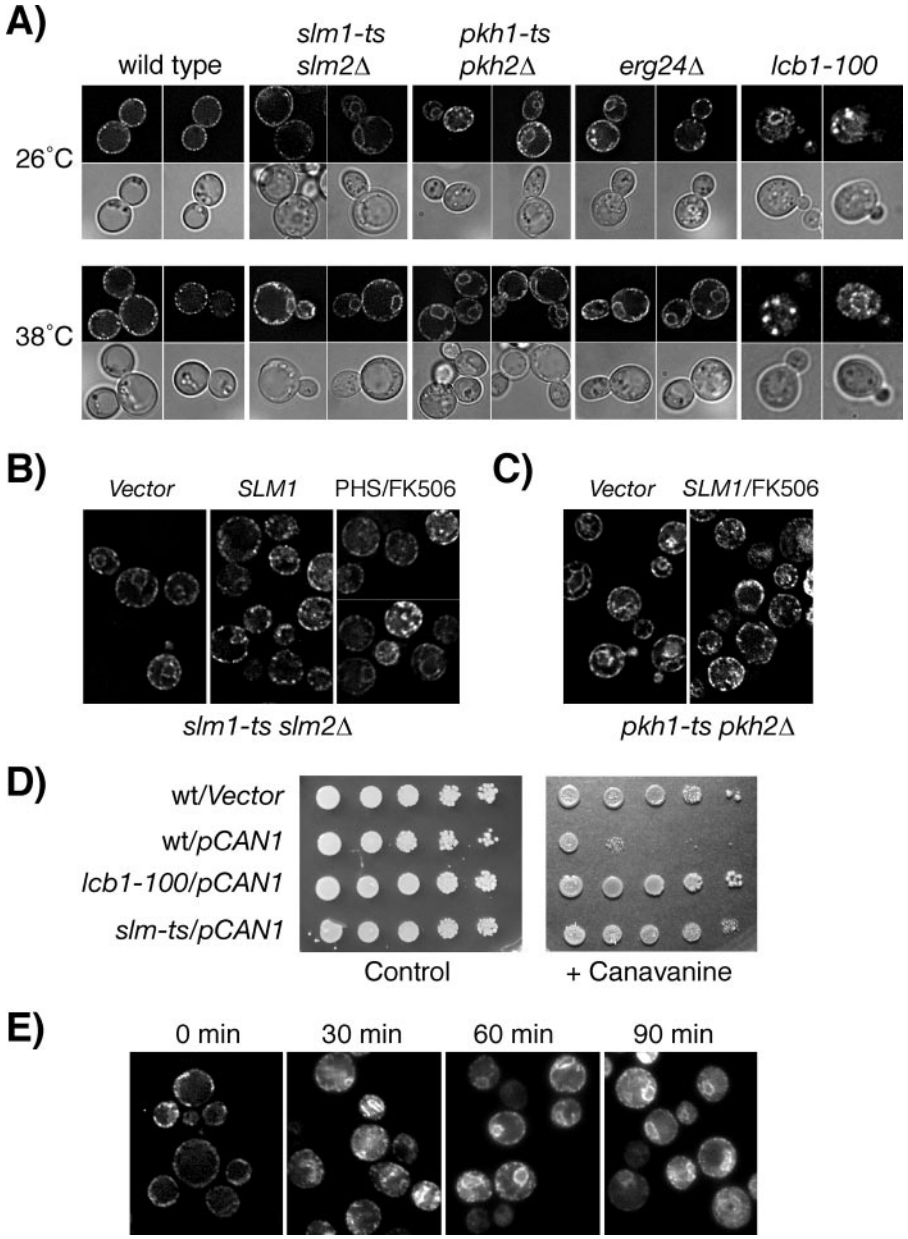

FIG. 10. Loss of Slm function results in defective delivery of the arginine transporter Can1 to the plasma membrane. (A) A plasmid encoding Can1p-GFP was expressed in wt (W303), *slm1-ts slm2*Δ, *pkh1-ts pkh2*Δ, *erg24*Δ, and *lcb1-100* strains and Can1-GFP was visualized in living cells grown at the permissive (26°C) or nonpermissive (38°C) temperature for 1 h. Representative examples of GFP localization are shown. GFP signal is shown in the top panels; DIC images of the same cells are shown in the bottom panels. (B) Can1-GFP localization in *slm1-ts slm2*Δ mutant cells (strain JK515) containing empty vector (left and right panels) or *SLM1* expressed from a high-copy-number vector under the control of the *GPD* promoter (2μm, *TRP1*; middle panel). Cells were either left untreated or incubated in the presence of PHS (7.5 μM) and FK506 (2 μg/ml) for 1 h at 26°C before being shifted to 38°C for 2 h, and GFP fluorescence was visualized. (C) Can1-GFP localization is shown in *pkh1-ts pkh2*Δ mutant cells containing empty vector (left panel) or *SLM1* expressed from a high-copy-number vector under the control of the GPD promoter (2μm, *TRP1*; right panel). Vector-transformed cells were left untreated, whereas cells expressing *SLM1* were incubated in the presence of FK506 (2 μg/ml) for 1 h at 26°C before being shifted to 38°C for 2 h, and GFP fluorescence was visualized. (D) Serial dilutions of wild-type (W303), *lcb1-100*, and *slm1-ts slm2*Δ (JK515) strains transformed with empty vector or p*CAN1-GFP* were plated on media lacking Arg to verify plating (left panel) and on medium lacking Arg and containing the arginine analog canavanine (0.5 μg/ml). Plates were incubated at 30°C for 3 days. (E) Wild-type cells (W303) containing a plasmid encoding for Can1p-GFP were treated with latrunculin A (5 μM) at 30°C, and GFP fluorescence in living cells was recorded at the indicated times.

DISCUSSION

The related PH domain-containing proteins Slm1 and Slm2 were originally identified as effectors of the $PI4,5P_2$ and TORC2 signaling pathways and shown to be essential for growth and actin polarization (3, 20). The studies presented here extend these earlier observations and demonstrate that Slm proteins are also targets of sphingolipid-dependent signaling. We show that Slm1 is essential for growth and proper actin

polarization under conditions where de novo sphingolipid synthesis is compromised, suggesting that Slm proteins and sphingolipids cooperate to promote cell survival. Our results further establish a role for sphingolipid signaling pathways in modulating Slm function during heat stress. One role of sphingolipids may be to indirectly modulate Slm activity by regulating $PI4,5P_2$ synthesis required for Slm1 and Slm2 plasma membrane targeting (34). However, a second, essential role of the sphingolipid-activated signaling pathway is to stimulate Slm phosphorylation on both serine and threonine residues and this phosphorylation event is vital for survival under heat stress conditions.

Sphingolipids signaling is specifically induced in response to heat stress in yeast and the kinetics of Slm phosphorylation correlate well with heat-induced changes in sphingoid base metabolites. Heat stress induces a rapid increase in the sphingoid bases PHS and DHS. This increase is transient; levels peak after 10 to 15 min, returning to basal levels within 60 min (19, 32). PHS and DHS are rapidly metabolized to PHS-1P and DHS-1P, which peak 15 min after heat stress (21, 52) followed after approximately 1 h by an increase in ceramide metabolites via de novo synthesis (58). Thus, PHS or a PHS metabolite may promote Slm phosphorylation by activating an upstream kinase. Consistent with such an idea, we found that Slm phosphorylation levels are significantly diminished in a yeast mutant defective for the sphingoid base-activated kinases Pkh1 and Pkh2, suggesting that the Pkh signaling cascade regulates Slm function. Slm1 and Slm2 lack canonical consensus Pkh/PDK1 phosphorylation motifs, which are present in all known Pkh targets (9, 29). In agreement with this, Pkh1 failed to directly phosphorylate Slm proteins in vitro. Thus, Slm1 and Slm2 phosphorylation involves an as-yet-unidentified kinase whose activity is modulated by the Pkh signaling cascade. Pkh kinases are known to directly activate several kinases, including Pkc1p, Sch9, and the related kinases Ypk1 and Ypk2. Our data thus far exclude Ypk1/2, and it remains to be determined which kinase(s) directly phosphorylates Slm1/2.

Heat-induced Slm1 phosphorylation is, at least in part, counteracted by the Ca^{2+}/calmodulin-dependent protein phosphatase calcineurin. We show that Slm1 and Slm2 both physically interact with Cna1 via a calcineurin docking site present in their C termini and that deletion of this calcineurin-binding site in Slm1 or treatment of yeast cells with the calcineurin inhibitor FK506 increases basal levels of Slm phosphorylation on both serine and threonine residues. Interestingly, calcineurin activation in an early phase of the heat shock response may also be mediated by sphingolipids (PHS-1P) through stimulation of Ca^{2+} influx. Thus, sphingolipids may modulate Slm phosphorylation both positively and negatively during heat stress. PHS-1P may trigger the calcineurin-dependent dephosphorylation of Slm observed immediately following heat shock, whereas PHS stimulates Pkh-dependent rephosphorylation of Slm proteins during the recovery period. Together, our data suggest that Slm activity is modulated via a phosphorylation/dephosphorylation cycle with Pkh kinases and calcineurin antagonistically regulating Slm activity.

How does phosphorylation/dephosphorylation affect Slm function? The finding that the specific calcineurin inhibitor FK506 in combination with PHS can partially suppress the growth defect of the temperature-sensitive *slm1-ts slm2*Δ mutant at the nonpermissive temperature argues for a negative role of calcineurin in Slm regulation and a positive role of sphingolipids in enhancing Slm activity. Consistent with a negative role of calcineurin in Slm regulation, deletion of the calcineurin-binding site does not abolish Slm function. Accordingly, the $Slm1_{\Delta CN}$ mutant not only is functional and suppresses growth and actin defects of *slm1-ts slm2*Δ mutant cells at 38°C (data not shown) but also is more effective than wild-type *SLM1* in restoring proper actin polarization in *pkh* mutant cells.

Our data further demonstrate that phospho-Slm plays a critical role during heat stress and is required for maintaining cell survival and proper actin polarization. This conclusion is supported by biochemical and genetic data showing that conditions that enhance Slm phosphorylation (treatment of cells with FK506 and PHS) also suppress the lethality and actin defects associated with loss of Slm function. Furthermore, identification and functional characterization of one heat-induced phosphorylation site in Slm1, Ser_{659}, using mass spectroscopic analysis and mutagenesis studies directly implicates phosphorylation in survival during heat stress. Replacement of Ser_{659} in Slm1 with Ala, which prevents phosphorylation, affects Slm1 function under heat shock conditions only. Accordingly, while this Slm1 variant can complement lethality of the *slm1-ts slm2*Δ mutant under physiological growth conditions (30°C), it fails to do so at 38°C. Thus, phosphorylation may increase Slm1 activity or promote interaction with a cellular component necessary for maintaining growth and proper actin polarization under environmental stress conditions. In agreement with such a hypothesis, the $Slm1_{Ser659D}$ mutant appears to be hyperactive in vivo compared to the wild-type protein. Due to the close proximity of Ser_{659} to the calcineurin binding site (amino acids 668 to 682), it is tempting to speculate that Ser_{659} is the site dephosphorylated by calcineurin. Further studies, however, are needed to determine the identity of the residues dephosphorylated by calcineurin and its relation to Ser_{659}.

Sphingolipid-dependent activation of the Pkh pathway is essential for growth, and activated Pkh kinases modulate at least two essential signaling branches required for cell wall synthesis and actin polarization. Our genetic and biochemical studies suggest that Slm proteins function as effectors in one Pkh-regulated signaling branch or act in a parallel, functionally redundant pathway. Perhaps more in favor of the former, we found that an increased dosage of *SLM1* can partially rescue the growth and actin cytoskeleton organization defects of the temperature-sensitive *pkh1-ts pkh2*Δ cells when these cells are osmotically stabilized. Conversely, an increased dosage of *PKH1* suppressed neither the growth nor actin defects of the *slm1-ts slm2*Δ mutant at nonpermissive temperature (data not shown). In agreement with the notion that the Pkh signaling cascade stimulates Slm activity, mutations that enhance or mimic phosphorylation ($Slm1_{Ser659D}$ and $Slm1_{\Delta CN}$) confer an enhanced ability to suppress the growth and actin defects of *pkh1-ts pkh2*Δ mutant cells. Together, our data are most compatible with a model in which Slm proteins function in a branch of the Pkh signaling pathway to promote actin polarization during heat stress.

Finally, our studies suggest that Slm proteins are required for aspects of sphingolipid-dependent transport processes, be-

cause delivery of the arginine permease Can1 to the plasma membrane, which is dependent on de novo sphingolipid synthesis, is blocked in cells lacking Slm activity. In yeast, ongoing sphingolipid biosynthesis is required for the formation of lipid raft domains in the ER and may play a role in the fusion of COPII vesicles with *cis*-Golgi membranes (51). The defect in ER exit of Can1 in *slm-ts* mutants would thus be consistent with a common role of Slm proteins and sphingolipids in protein delivery to lipid raft microdomains. Interestingly, plasma membrane delivery of the lipid raft-associated protein Pma1 appeared not to be significantly affected in *slm1-ts slm2*Δ mutants. The reason for the intracellular retention of Can1 only is currently unknown, but it may be due to the preferential association of Can1 and Pma1 with raft domains of different lipid compositions along the secretory pathway (45) and at the plasma membrane (39). Can1 is thought to associate with raft domains in the ER (45), whereas Pma1 raft association has been proposed to occur predominantly in the Golgi apparatus (4, 35). Thus, Can1 and Pma1 may be transported via different subpopulations of vesicles that are differentially sensitive to loss of Slm function. In support of such a hypothesis, immunofluorescence studies revealed more significant overlap of Slm1 signal with Can1 and Sur7, compared to Pma1 (Fig. S1). Thus, Slm proteins may play a role in the trafficking of Can1/Sur7-containing vesicles and their targeting to specific membrane domains at the plasma membrane. Additional studies will need to address this issue.

Slm1 and Slm2 were previously implicated in vesicular trafficking to the cell surface, and several proteins, including the Rab-type GTPase Sec4 and the v-SNARE Snc1, necessary for fusion of secretory vesicles with the plasma membrane, were mislocalized in *slm1-ts slm2*Δ mutants (3). While the precise role of Slm proteins in the exocytotic pathway is not known, there is precedence for a functional connection between Snc1 and sphingolipid biosynthesis in this process. Sphingoid bases and ceramides can modulate secretion and endocytic recycling functions of the redundant v-SNAREs Snc1 and Snc2, because addition of exogenous PHS to the growth medium can restore Golgi-to-plasma membrane transport in yeast mutants defective for Snc1/2 and the t-SNAREs Sso1/2 (41). In addition, the growth defect of the *snc1*Δ *snc2*Δ mutant can also be suppressed by altering the availability of different ceramide precursors (14, 43). How alterations in sphingolipids suppress the sorting defects of the *snc1*Δ *snc2*Δ mutant is unclear, but it could be due to changes in sphingolipid signaling or membrane curvature and fluidity. Perhaps in support of a signaling mechanism, we found that the Can1 transport defect is phenocopied by a yeast mutant defective in Pkh function, suggesting that Pkh kinases and Slm proteins affect Can1 trafficking by a common mechanism. The role of Slm proteins and Pkh1/2 kinases in Can1 plasma membrane delivery may be dependent on their roles in regulating actin cytoskeletal polarization, because intracellular retention of Can1 is also observed upon disruption of actin filaments by latrunculin A. While the precise mechanism by which Slm proteins affects Can1 transport remains to be determined, our studies suggest that Slm proteins act downstream of a sphingolipid-derived signal to control the organization of the actin cytoskeleton in response to heat stress. Thus, Slm proteins are subject to control by multiple signaling pathways, including $PI4,5P_2$ TorC2 and sphingolipid-activated Pkh kinases, and it will be interesting to determine whether and how input of these different signals is integrated to temporally and spatially affect actin organization.

ACKNOWLEDGMENTS

We thank Sandra K. Lemmon, Kunihiro Matsumoto, Widmar Tanner, and Jeremy Thorner for their generous gifts of strains and plasmids, Eric Chang for the gift of canavanine and latrunculin A, and Felicity Ashcroft for comments on the manuscript.

This work was supported by grants GM068098 and GM068098-S1 from the National Institutes of Health and grant 0555128Y from the American Heart Association.

This article is dedicated to the memory of Sarah Leigh Rodgerson.

ADDENDUM

While the manuscript was in review, two other papers were published (8, 54) reporting a role of Slm proteins in sphingolipid metabolism (54) and the regulation of calcineurin activity (54), as well as the modulation of Slm phosphorylation by sphingolipids and calcineurin (8). Our data demonstrating antagonistic roles of sphingolipids and calcineurin in the modulation of Slm phosphorylation are in good agreement with a study by Bultynck et al. (8). In addition, a role of Slm proteins in the maintenance of normal cellular sphingolipid levels and downregulation of calcineurin activity, as reported by Tabuchi et al. (54), may explain, in part, the Can1 trafficking and actin defects observed in *slm* mutants.

REFERENCES

1. **Audhya, A., and S. D. Emr.** 2002. Stt4 PI 4-kinase localizes to the plasma membrane and functions in the Pkc1-mediated MAP kinase cascade. Dev. Cell **2:**593–605.
2. **Audhya, A., M. Foti, and S. D. Emr.** 2000. Distinct roles for the yeast phosphatidylinositol 4-kinases, Stt4p and Pik1p, in secretion, cell growth, and organelle membrane dynamics. Mol. Biol. Cell **11:**2673–2689.
3. **Audhya, A., R. Loewith, A. B. Parsons, L. Gao, M. Tabuchi, H. Zhou, C. Boone, M. N. Hall, and S. D. Emr.** 2004. Genome-wide lethality screen identifies new $PI4,5P_2$ effectors that regulate the actin cytoskeleton. EMBO J. **23:**3747–3757.
4. **Bagnat, M., S. Keranen, A. Shevchenko, and K. Simons.** 2000. Lipid rafts function in biosynthetic delivery of proteins to the cell surface in yeast. Proc. Natl. Acad. Sci. USA **97:**3254–3259.
5. **Beeler, T., D. Bacikova, K. Gable, L. Hopkins, C. Johnson, H. Slife, and T. Dunn.** 1998. The Saccharomyces cerevisiae TSC10/YBR265w gene encoding 3-ketosphinganine reductase is identified in a screen for temperature-sensitive suppressors of the Ca2+-sensitive csg2Delta mutant. J. Biol. Chem. **273:**30688–30694.
6. **Beeler, T. J., D. Fu, J. Rivera, E. Monaghan, K. Gable, and T. M. Dunn.** 1997. SUR1 (CSG1/BCL21), a gene necessary for growth of Saccharomyces cerevisiae in the presence of high Ca2+ concentrations at 37°C, is required for mannosylation of inositolphosphorylceramide. Mol. Gen. Genet. **255:** 570–579.
7. **Birchwood, C. J., J. D. Saba, R. C. Dickson, and K. W. Cunningham.** 2001. Calcium influx and signaling in yeast stimulated by intracellular sphingosine 1-phosphate accumulation. J. Biol. Chem. **276:**11712–11718.
8. **Bultynck, G., V. L. Heath, A. P. Majeed, J. M. Galan, R. Haguenauer-Tsapis, and M. S. Cyert.** 2006. Slm1 and Slm2 are novel substrates of the calcineurin phosphatase required for heat stress-induced endocytosis of the yeast uracil permease. Mol. Cell. Biol. **26:**4729–4745.
9. **Casamayor, A., P. D. Torrance, T. Kobayashi, J. Thorner, and D. R. Alessi.** 1999. Functional counterparts of mammalian protein kinases PDK1 and SGK in budding yeast. Curr. Biol. **9:**186–197.
10. **Chung, N., G. Jenkins, Y. A. Hannun, J. Heitman, and L. M. Obeid.** 2000. Sphingolipids signal heat stress-induced ubiquitin-dependent proteolysis. J. Biol. Chem. **275:**17229–17232.
11. **Cowart, L. A., Y. Okamoto, F. R. Pinto, J. L. Gandy, J. S. Almeida, and Y. A. Hannun.** 2003. Roles for sphingolipid biosynthesis in mediation of specific programs of the heat stress response determined through gene expression profiling. J. Biol. Chem. **278:**30328–30338.
12. **Cyert, M. S.** 2003. Calcineurin signaling in Saccharomyces cerevisiae: how yeast go crazy in response to stress. Biochem. Biophys. Res. Commun. **311:**1143–1150.

13. **Cyert, M. S., R. Kunisawa, D. Kaim, and J. Thorner.** 1991. Yeast has homologs (CNA1 and CNA2 gene products) of mammalian calcineurin, a calmodulin-regulated phosphoprotein phosphatase. Proc. Natl. Acad. Sci. USA **88:**7376–7380.
14. **David, D., S. Sundarababu, and J. E. Gerst.** 1998. Involvement of long chain fatty acid elongation in the trafficking of secretory vesicles in yeast. J. Cell Biol. **143:**1167–1182.
15. **Desrivieres, S., F. T. Cooke, H. Morales-Johansson, P. J. Parker, and M. N. Hall.** 2002. Calmodulin controls organization of the actin cytoskeleton via regulation of phosphatidylinositol (4,5)-bisphosphate synthesis in Saccharomyces cerevisiae. Biochem. J. **366:**945–951.
16. **Desrivieres, S., F. T. Cooke, P. J. Parker, and M. N. Hall.** 1998. MSS4, a phosphatidylinositol-4-phosphate 5-kinase required for organization of the actin cytoskeleton in Saccharomyces cerevisiae. J. Biol. Chem. **273:**15787–15793.
17. **Dickson, R. C.** 1998. Sphingolipid functions in Saccharomyces cerevisiae: comparison to mammals. Annu. Rev. Biochem. **67:**27–48.
18. **Dickson, R. C., and R. L. Lester.** 2002. Sphingolipid functions in Saccharomyces cerevisiae. Biochim. Biophys. Acta **1583:**13–25.
19. **Dickson, R. C., E. E. Nagiec, M. Skrzypek, P. Tillman, G. B. Wells, and R. L. Lester.** 1997. Sphingolipids are potential heat stress signals in Saccharomyces. J. Biol. Chem. **272:**30196–30200.
20. **Fadri, M., A. Daquinag, S. Wang, T. Xue, and J. Kunz.** 2005. The pleckstrin homology domain proteins Slm1 and Slm2 are required for actin cytoskeleton organization in yeast and bind phosphatidylinositol-4,5-bisphosphate and TORC2. Mol. Biol. Cell **16:**1883–1900.
21. **Ferguson-Yankey, S. R., M. S. Skrzypek, R. L. Lester, and R. C. Dickson.** 2002. Mutant analysis reveals complex regulation of sphingolipid long chain base phosphates and long chain bases during heat stress in yeast. Yeast **19:**573–586.
22. **Friant, S., R. Lombardi, T. Schmelzle, M. N. Hall, and H. Riezman.** 2001. Sphingoid base signaling via Pkh kinases is required for endocytosis in yeast. EMBO J. **20:**6783–6792.
23. **Friant, S., B. Zanolari, and H. Riezman.** 2000. Increased protein kinase or decreased PP2A activity bypasses sphingoid base requirement in endocytosis. EMBO J. **19:**2834–2844.
24. **Futerman, A. H., and Y. A. Hannun.** 2004. The complex life of simple sphingolipids. EMBO Rep. **5:**777–782.
25. **Gould, K. L., L. Ren, A. S. Feoktistova, J. L. Jennings, and A. J. Link.** 2004. Tandem affinity purification and identification of protein complex components. Methods **33:**239–244.
26. **Hearn, J. D., R. L. Lester, and R. C. Dickson.** 2003. The uracil transporter Fur4p associates with lipid rafts. J. Biol. Chem. **278:**3679–3686.
27. **Ho, H. L., Y. S. Shiau, and M. Y. Chen.** 2005. Saccharomyces cerevisiae TSC11/AVO3 participates in regulating cell integrity and functionally interacts with components of the Tor2 complex. Curr. Genet. **47:**273–288.
28. **Homma, K., S. Terui, M. Minemura, H. Qadota, Y. Anraku, Y. Kanaho, and Y. Ohya.** 1998. Phosphatidylinositol-4-phosphate 5-kinase localized on the plasma membrane is essential for yeast cell morphogenesis. J. Biol. Chem. **273:**15779–15786.
29. **Inagaki, M., T. Schmelzle, K. Yamaguchi, K. Irie, M. N. Hall, and K. Matsumoto.** 1999. PDK1 homologs activate the Pkc1-mitogen-activated protein kinase pathway in yeast. Mol. Cell. Biol. **19:**8344–8352.
30. **Ito, H., Y. Fukuda, K. Murata, and A. Kimura.** 1983. Transformation of intact yeast cells treated with alkali cations. J. Bacteriol. **153:**163–168.
31. **Ito, T., T. Chiba, R. Ozawa, M. Yoshida, M. Hattori, and Y. Sakaki.** 2001. A comprehensive two-hybrid analysis to explore the yeast protein interactome. Proc. Natl. Acad. Sci. USA **98:**4569–4574.
32. **Jenkins, G. M., A. Richards, T. Wahl, C. Mao, L. Obeid, and Y. Hannun.** 1997. Involvement of yeast sphingolipids in the heat stress response of Saccharomyces cerevisiae. J. Biol. Chem. **272:**32566–32572.
33. **Jung, S. Y., A. Malovannaya, J. Wei, B. W. O'Malley, and J. Qin.** 2005. Proteomic analysis of steady-state nuclear hormone receptor coactivator complexes. Mol. Endocrinol. **19:**2451–2465.
34. **Kobayashi, T., H. Takematsu, T. Yamaji, S. Hiramoto, and Y. Kozutsumi.** 2005. Disturbance of sphingolipid biosynthesis abrogates the signaling of Mss4, phosphatidylinositol-4-phosphate 5-kinase, in yeast. J. Biol. Chem. **280:**18087–18094.
35. **Lee, M. C., S. Hamamoto, and R. Schekman.** 2002. Ceramide biosynthesis is required for the formation of the oligomeric H+-ATPase Pma1p in the yeast endoplasmic reticulum. J. Biol. Chem. **277:**22395–22401.
36. **Liu, J.** 1993. FK506 and cyclosporin, molecular probes for studying intracellular signal transduction. Immunol. Today **14:**290–295.
37. **Liu, K., X. Zhang, R. L. Lester, and R. C. Dickson.** 2005. The sphingoid long chain base phytosphingosine activates AGC-type protein kinases in Saccharomyces cerevisiae including Ypk1, Ypk2, and Sch9. J. Biol. Chem. **280:**22679–22687.
38. **Luo, C., K. T. Shaw, A. Raghavan, J. Aramburu, F. Garcia-Cozar, B. A. Perrino, P. G. Hogan, and A. Rao.** 1996. Interaction of calcineurin with a domain of the transcription factor NFAT1 that controls nuclear import. Proc. Natl. Acad. Sci. USA **93:**8907–8912.
39. **Malinska, K., J. Malinsky, M. Opekarova, and W. Tanner.** 2004. Distribution of Can1p into stable domains reflects lateral protein segregation within the plasma membrane of living S. cerevisiae cells. J. Cell Sci. **117:**6031–6041.
40. **Malinska, K., J. Malinsky, M. Opekarova, and W. Tanner.** 2003. Visualization of protein compartmentation within the plasma membrane of living yeast cells. Mol. Biol. Cell **14:**4427–4436.
41. **Marash, M., and J. E. Gerst.** 2001. t-SNARE dephosphorylation promotes SNARE assembly and exocytosis in yeast. EMBO J. **20:**411–421.
42. **Nagiec, M. M., M. Skrzypek, E. E. Nagiec, R. L. Lester, and R. C. Dickson.** 1998. The LCB4 (YOR171c) and LCB5 (YLR260w) genes of Saccharomyces encode sphingoid long chain base kinases. J. Biol. Chem. **273:**19437–19442.
43. **Oh, C. S., D. A. Toke, S. Mandala, and C. E. Martin.** 1997. ELO2 and ELO3, homologues of the Saccharomyces cerevisiae ELO1 gene, function in fatty acid elongation and are required for sphingolipid formation. J. Biol. Chem. **272:**17376–17384.
44. **Ono, B. I., Y. Ishino, and S. Shinoda.** 1983. Nonsense mutations in the can1 locus of Saccharomyces cerevisiae. J. Bacteriol. **154:**1476–1479.
45. **Opekarova, M., K. Malinska, L. Novakova, and W. Tanner.** 2005. Differential effect of phosphatidylethanolamine depletion on raft proteins: further evidence for diversity of rafts in Saccharomyces cerevisiae. Biochim. Biophys. Acta **1711:**87–95.
46. **Roelants, F. M., P. D. Torrance, N. Bezman, and J. Thorner.** 2002. Pkh1 and pkh2 differentially phosphorylate and activate ypk1 and ykr2 and define protein kinase modules required for maintenance of cell wall integrity. Mol. Biol. Cell **13:**3005–3028.
47. **Roelants, F. M., P. D. Torrance, and J. Thorner.** 2004. Differential roles of PDK1- and PDK2-phosphorylation sites in the yeast AGC kinases Ypk1, Pkc1 and Sch9. Microbiology **150:**3289–3304.
48. **Schmidt, A., J. Kunz, and M. N. Hall.** 1996. TOR2 is required for organization of the actin cytoskeleton in yeast. Proc. Natl. Acad. Sci. USA **93:**13780–13785.
49. **Sherman, F., G. R. Fink, and J. B. Hicks.** 1983. Methods in yeast genetics. Cold Spring Harbor Laboratory Press, Cold Spring Harbor, N.Y.
50. **Simons, K., and E. Ikonen.** 1997. Functional rafts in cell membranes. Nature **387:**569–572.
51. **Skrzypek, M., R. L. Lester, and R. C. Dickson.** 1997. Suppressor gene analysis reveals an essential role for sphingolipids in transport of glycosylphosphatidylinositol-anchored proteins in Saccharomyces cerevisiae. J. Bacteriol. **179:**1513–1520.
52. **Skrzypek, M. S., M. M. Nagiec, R. L. Lester, and R. C. Dickson.** 1999. Analysis of phosphorylated sphingolipid long-chain bases reveals potential roles in heat stress and growth control in Saccharomyces. J. Bacteriol. **181:**1134–1140.
53. **Sun, Y., R. Taniguchi, D. Tanoue, T. Yamaji, H. Takematsu, K. Mori, T. Fujita, T. Kawasaki, and Y. Kozutsumi.** 2000. Sli2 (Ypk1), a homologue of mammalian protein kinase SGK, is a downstream kinase in the sphingolipid-mediated signaling pathway of yeast. Mol. Cell. Biol. **20:**4411–4419.
54. **Tabuchi, M., A. Audhya, A. B. Parsons, C. Boone, and S. D. Emr.** 2006. The phosphatidylinositol 4,5-biphosphate and TORC2 binding proteins Slm1 and Slm2 function in sphingolipid regulation. Mol. Cell. Biol. **26:**5861–5875.
55. **Takenawa, T., and T. Itoh.** 2001. Phosphoinositides, key molecules for regulation of actin cytoskeletal organization and membrane traffic from the plasma membrane. Biochim. Biophys. Acta **1533:**190–206.
56. **Uemura, S., A. Kihara, J. Inokuchi, and Y. Igarashi.** 2003. Csg1p and newly identified Csh1p function in mannosylinositol phosphorylceramide synthesis by interacting with Csg2p. J. Biol. Chem. **278:**45049–45055.
57. **Uetz, P., L. Giot, G. Cagney, T. A. Mansfield, R. S. Judson, J. R. Knight, D. Lockshon, V. Narayan, M. Srinivasan, P. Pochart, A. Qureshi-Emili, Y. Li, B. Godwin, D. Conover, T. Kalbfleisch, G. Vijayadamodar, M. Yang, M. Johnston, S. Fields, and J. M. Rothberg.** 2000. A comprehensive analysis of protein-protein interactions in Saccharomyces cerevisiae. Nature **403:**623–627.
58. **Wells, G. B., R. C. Dickson, and R. L. Lester.** 1998. Heat-induced elevation of ceramide in Saccharomyces cerevisiae via de novo synthesis. J. Biol. Chem. **273:**7235–7243.
59. **Yin, H. L., and P. A. Janmey.** 2003. Phosphoinositide regulation of the actin cytoskeleton. Annu. Rev. Physiol. **65:**761–789.
60. **Zanolari, B., S. Friant, K. Funato, C. Sutterlin, B. J. Stevenson, and H. Riezman.** 2000. Sphingoid base synthesis requirement for endocytosis in Saccharomyces cerevisiae. EMBO J. **19:**2824–2833.
61. **Zhao, C., T. Beeler, and T. Dunn.** 1994. Suppressors of the Ca^{2+}-sensitive yeast mutant (csg2) identify genes involved in sphingolipid biosynthesis. Cloning and characterization of SCS1, a gene required for serine palmitoyltransferase activity. J. Biol. Chem. **269:**21480–21488.